ABSTRACT

Xia, Heng. Effects of Medium Access Control on the Capacity of Mobile Ad Hoc Networks. (Under the direction of Dr. Wenye Wang).

As various wireless networks evolves into the next generation to provide better services, a key technology, mobile ad hoc networks (MANETs), has emerged recently. The dynamic topology, multi-hop transmission, and the nature of wireless channels create many challenging research topics in the area of MANETs. Recently, there has been work on determining the capacity of MANETs. The effects of some factors, such as node mobility, number of nodes, and transmission range, on the capacity of MANETs have been considered. In this work, we define and investigate the capacity of MANETs, considering the effects of medium access control (MAC). Since all the nodes in MANETs use a single or multiple channels to communicate, MAC plays an important role in coordinating channel access among nodes so that information gets through from one node to another. The MAC affects the capacity of MANETs in two aspects: collisions and spatial reuse. Three basic mechanisms are adopted to eliminate the incidence of collisions and maximize spatial reuse, i.e., carrier sense, handshake, and back-off. We define and use persistent probability, sensing range and back-off time to represent the effect of these mechanisms. The characteristics of MAC are thoroughly examined and an analytical solution for capacity evaluation is proposed. Numerical results are presented to demonstrate the effects of MAC, including carrier sense, handshake and back-off mechanism on the capacity of MANETs in terms of persistent probability, sensing range, and back-off time.

Effects of Medium Access Control on the Capacity of Mobile Ad Hoc Networks

by

Heng Xia

A thesis submitted to the Graduate Faculty of
North Carolina State University
in partial satisfaction of the
requirements for the Degree of
Master of Science

Department of Electrical and Computer Engineering

Raleigh

2005

Approved By:

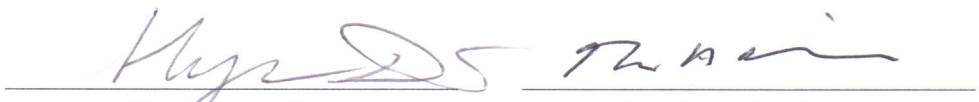

Dr. Huaiyu Dai

Dr. Arne A. Nilsson

Dr. Wenye Wang
Chair of Advisory Committee

To my parents ...

Biography

Heng Xia was born in China in 1981. He graduated from Xi'an Jiaotong University, Xi'an in July 2003 with a bachelor's degree in Electrical Engineering. He then came to North Carolina State University, Raleigh for the Master of Science degree in Electrical Engineering.

Acknowledgements

I would like to specially thank my advisor and committee chair, Dr. Wenye Wang for her valuable help and guidance. I would like to thank her for her patience and support throughout this process. This work would not have been done without her careful guidance. I would also like to thank my committee members, Dr. Arne A. Nilsson and Dr. Huaiyu Dai for their support and helpful comments and feedback.

I am grateful for the support I have always received from my parents. Lastly, I would like to thank all my friends who have always been there for me.

Contents

List of Figures

List of Tables

Chapter 1

Introduction

The mobile ad hoc network (MANET) has become a hot research area in the recent few years. It provides a flexible access method and is applied in many areas where traditional networks cannot work. In the design of MANETs, it is a meaningful topic to analyze its capacity considering the effects of different layers in the OSI (Open System Interconnect) model, defined by CCITT (International Telegraph and Telephone Consultative Committee) in 1984. In this thesis, the effects of MAC (Medium Access Control) on the capacity of MANETs are evaluated, since the capacity of MANETs mainly depends on the performance of MAC layer [3]. As the introduction of our work, this chapter presents an overview of MANETs and the MAC layer. Also, we present an overview of existing capacity analysis for MANETs and show how MAC plays a key role to the capacity of MANETs.

1.1 Overview of Mobile Ad Hoc Networks

An MANET is a self-configuring network of mobile nodes connected by wireless links, and the union of the nodes and links form an arbitrary topology. The nodes are free to move randomly and organize themselves arbitrarily; thus, the network's wireless

topology may change rapidly and unpredictably. Such a network may operate in a stand-alone fashion, or may be connected to the larger Internet.

The earliest MANETs were called "packet radio" networks, sponsored by DARPA (Defense Advanced Research Projects Agency) in the early 1970s, and was supposed to be perfect for the battlefield where there is usually no infrastructure for communication at all. It is interesting to note that these early packet radio systems predated the Internet, and indeed were part of the motivation of the original Internet Protocol suite. Although the past MANETs were designed primarily for military utility, current MANETs are applied in more areas. Today one of the most popular scenarios is the communication within groups of people with laptops and other hand-held devices. Another scenario is the communication networks for supporting rescue personnel in disaster areas after an earthquake or the similar [1, 48].

Nodes in an MANET are not only mobile but may have limited capabilities and may be interested in participating in the network only for a short period of time. This behavior gives rise to a number of interesting features.

1. **Dynamic Topology.** Nodes may voluntarily join or leave an MANET at any time. Also, nodes may lose battery power or fail or decide to shut down at any time. Each node has a wireless *transmission range* which is the range within which any node can correctly decode the received signal if there is no interference. A node or a group of nodes may move out of transmission range of other nodes at any time, thus partitioning the network. Similarly, node movement may cause two partitions to be reconnected, thus merging the partitions. Thus, the topology and membership of an MANET is dynamic in nature. Hence, any protocols for MANETs which make use of centralized nodes are prone to failure. In order for a protocol for MANETs to be robust in the face of continual change, it should be distributed in nature [28, 39].

2. **Multi-hop Transmissions.** If two nodes are within the wireless transmission range of each other, they can communicate directly. Otherwise, intermediate nodes must forward packets between the two nodes. The situation here is different from that in wired networks. In conventional wired networks, only a few nodes are needed as

routers to forward packets from source nodes to destination nodes. Given the highly dynamic nature of MANETs, it would not be suitable for a few nodes to function as routers. These router nodes could move or leave the network or shut down (voluntarily or involuntarily) at any time. Hence in MANETs, every node has knowledge of routes to other nodes in the network. Thus, each node acts as a router and participates in routing a packet to its destination [39].

3. **Open Medium.** All the mobile nodes in MANETs use the same frequency spectrum (or physical channel), therefore, MAC plays an important role in coordinating channel access among the nodes so that information gets through from one node to another. Hence the MAC layer protocols for MANETs must differ from those for wired networks in which the nodes are fixed and the channel is reliable. Due to dynamic topology and multi-hop transmissions in MANETs, although many MAC layer protocols were proposed for wireless networks such as Carrier Sense Multiple Access (CSMA) protocol and IEEE 802.11 MAC protocol, few of them can be directly applied to MANETs. Recently, a number of MAC schemes have been proposed for MANETs to address various relevant issues. In this thesis, we will discuss the mechanisms of these MAC schemes, and analyze the effects of these mechanisms on the capacity of MANETs.

There are some other features of MANETs in physical layer, transport layer, network layer, etc. They are beyond the discussion of this thesis, so we simply list them here. Next we will give an introduction about the capacity and MAC protocols for MANETs.

1.2 Capacity of MANETs

The capacity of an MANET is the measure of the ability that an MANET transmits and receives. It is affected by many factors such as network architecture, network topology, traffic pattern, network node density, number of channels used for each node, transmission power level, and node mobility [2]. These factors are determined once an MANET is set up, and thus are not adjustable in a certain period of time. With these factors given, the

capacity of MANETs is only affected by the protocol stack used in the network. The main focus of the analytical evaluation for the capacity of MANETs is on the physical layer, the MAC layer, and the network layer. If the analysis of MANETs is considered, the physical layer discussions share ground with research on other kinds of wireless networks, e.g., cellular networks. The MAC and network layers are more specific to MANETs and they are the distinguishing features of MANETs. Since the MAC layer has a direct bearing on how reliably and efficiently data can be transmitted between two nodes along the routing path in the network, the performance of the network layer relies on the MAC layer specifications. Therefore, the analysis of MAC layer can be considered a key to capacity evaluation of MANETs.

1.3 Medium Access Control in MANETs

Since MANETs have unique features compared to other wireless networks such as wireless local area networks (WLANs) and cellular networks, several challenges and issues on MAC protocol design come out. The first and most serious challenge is that the central control (such as base stations in cellular networks) usually is not available in MANETs due to the lack of infrastructure support. Without perfect coordination, collisions may take place when several nodes simultaneously access the shared channel, which will cause failed transmissions. Second, due to hardware constraints, a node cannot immediately detect collisions during its transmission, which leads to long transmission time and the waste of channel resource. Third, as every node in the network is moving around, the network topology changes frequently. Accordingly, each node may experience different degree of channel contention and collision. At the same time, the attendant route changes also affect the interaction between the MAC layer and higher layers. All of these challenges need to be carefully considered when designing MAC protocols for MANETs, in order to achieve the maximum capacity.

The primary goal of MAC is to coordinate the channel access among multiple nodes to achieve high channel utilization and high network capacity. In other words, The

coordination of channel access should minimize or eliminate the incidence of collisions and maximize spatial reuse at the same time [65].

1. **Collisions.** Collisions come from two aspects in MANETs. They may occur due to simultaneous transmissions by two or more nodes in a certain range where their packets collide and interfere with each other. Obviously, the more the active nodes in the range of a transmitter-receiver pair, the more severe the collisions.

   On the other hand, collisions can result from hidden terminals. A hidden terminal is the one that cannot sense an ongoing transmission of a transmitter so that can interfere with it by transmitting at the same time. As illustrated in Figure 1.1, node B is within the transmission range of node A, and thus within the sensing range of node A, but A and D are not in each other's sensing range. Here, the *sensing range* of a transmitter refers to a range within which any node can sense the received signal, whose power level exceeds a certain value referred to as sensing threshold. Let us consider the case where A is transmitting to B. Node D, being out of A's sensing range, cannot detect the signal and may therefore transmit to B, thus interfering with B's reception because signal to noise plus interference ratio (SINR) at B is not large enough for correct decoding. Hence D is a hidden terminal.

2. **Spatial Reuse.** To achieve high channel utilization, MAC also needs to maximize the spatial reuse. One way is to reduce the transmission power to allow more simultaneous transmissions in the networks. However, smaller transmission range means more transmission hops each packet needs to go through from source to destination. This, in turn, leads to heavier traffic at each node and could counteract the advantage of increased spatial reuse. Some literature [20, 23, 24] have already shown that there is a tradeoff between the spatial reuse and multiple forwardings in order to maximize the aggregate throughput in MANETs. In fact, the optimal transmission range depends on the number of nodes and their locations and moving speed and hence is difficult to achieve due to the dynamic and distributed nature of MANETs.

   Exposed terminal problem is another factor influencing the spatial reuse. An exposed

terminal is the one that can sense the transmission of a transmitter but cannot interfere with the reception at the receiver. However, it is not allowed to transmit simply because it senses a busy medium, which leads to bandwidth under-utilization. For example, in Figure 1.1, node E is the exposed terminal of A when A is transmitting to B. Since E is within A's sensing range, it senses A's transmission and decides to defer its own transmission. However, this is unnecessary because there is no way E's transmission can cause any collision at receiver B.

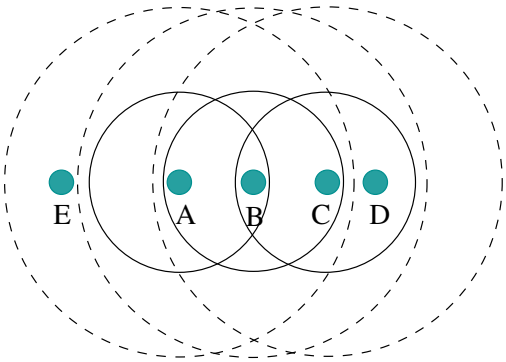

Figure 1.1: Illustration of the Hidden and Exposed Terminal Problems. (The solid and dashed circles denote the transmission and sensing ranges of node A, B, and C, respectively.)

Based on the above introduction, we can conclude that the MAC protocol in MANETs has some special needs other than the MAC protocols in WLANs and cellular networks:

1. Each node can transmit and receive packets directly from a peer node without a central coordination of the channel.

2. Overcome rising channel contention and collisions due to node mobility and lack of perfect coordination.

3. Overcome the hidden and exposed terminal problems which are more serious than WLANs and cellular networks.

A variety of MAC protocols have been proposed for MANETs, such as Carrier Sense Multiple Access (CSMA) [31], Medium Access Collision Avoidance (MACA) [29], MACA for Wireless LAN's (MACAW) [4], Floor Acquisition Multiple Access (FAMA) [18], 802.11 MAC [56], etc. We will give an investigation and comparison of these MAC protocols in Table 2.1 in Section 2.1.

1.4 Motivation and Contribution

As mentioned above, the motivation of this thesis is to find out how the MAC protocols affect the capacity of MANETs, which is not covered in the previous literature. Toward this goal, we first need to get insight of the MAC scheme of MANETs. Hence we discuss the basic components of MAC protocols, and study the solutions to the hidden and exposed terminal problems. Then we investigate the existing performance analysis of MAC and capacity analysis of MANETs. After that, we assume a specific MAC protocol for the use of our analysis, and propose the analytical models based on it. In our models, we consider the two fundamental issues in MAC, i.e., collisions and spatial reuse (Section 1.3), in terms of the persistent probability, sensing range, back-off time, and handshake mechanism. Subsequently, we carry out the capacity of MANETs, as a function of the sensing range, persistent probability and back-off time. At last, the effects of these factors on the capacity are examined with detailed numerical results.

1.5 Organization of the Thesis

The rest of the thesis is organized as follows. Chapter 2 provides the discussion of MAC protocols and overview of existing analysis of MAC and capacity of MANETs. In Chapter 3, we propose our analytical models under a certain handshake process and carry out the capacity of MANETs, considering the effects of the persistent probability, sensing range and back-off time. This chapter also gives the description of the heuristic procedure

to adjust the three parameters in order to achieve the maximum capacity. The numerical results of the capacity are discussed in Chapter 4. Finally, our conclusions and future work are presented in Chapter 5.

Chapter 2

Related Work on MAC Protocols and Capacity of MANETs

In this chapter, we first describe several basic components of contention-based MAC protocols in MANETs. Then we present some solutions to the classical hidden terminal and exposed terminal problems over MANETs. Finally, we investigate previous studies on the performance of MAC protocols.

2.1 MAC Protocols in MANETs

As we know, collisions can be quickly detected during the transmission in wired networks, such as the collision detection technique used in Ethernet. However, a transmitter cannot detect collisions when it transmits in wireless networks, and it relies on the receiver's acknowledgment to determine if any collision has occurred during the transmission. Obviously, if a long data packet encounters collisions, the resulting transmission period is quite long and undesirable. Therefore, how to effectively reduce collisions becomes a key issue

for MAC design in MANETs.

Several mechanisms have been proposed to avoid collisions in MAC, namely carrier sense, handshake, and back-off mechanism [65]. Carrier sense requires that a node transmit only if the channel is sensed idle. Multiple handshakes between the transmitter and receiver includes some short messages to avoid long collision time of data packets, and acknowledgements of successful transmissions. The back-off mechanism forces each node to wait for a random period before attempting the next transmission. In the following, we first introduce these mechanisms in the context of the IEEE 802.11 DCF (Distributed Coordination Function) protocol. Then, we discuss some schemes that outperform the 802.11 DCF by improving these mechanisms.

2.1.1 Carrier Sense, Back-off, and Handshake in the IEEE 802.11 DCF Protocol

IEEE 802.11 [56] Distributed Coordination Function (which is the specification for infrastructure-less mode in Wireless Ethernet) is a contention-based MAC protocol. To reduce the collision possibility, it uses carrier sense functions and binary exponential back-off (BEB) mechanism. In particular, two carrier sense functions, physical and virtual carrier sense functions, are used to determine the state of the channel. The former is provided by the physical layer and the latter by the MAC layer, which is also referred to as the network allocation vector (NAV). NAV predicts the duration that the channel will be busy in the future based on a duration information announced in transmitted packets. When either function indicates a busy channel, the channel is considered busy; otherwise, it is considered idle.

In the BEB mechanism, each node selects a random back-off timer uniformly distributed in $[0, CW - 1]$, where CW is the current contention window (CW) size. It decreases the back-off timer by one for each idle time slot, after waiting for a duration of DIFS (Distributed Inter-Frame Space) following a successful transmission, or EIFS (Extended Inter-Frame Space) following a bad or unknown frame. Transmission will restart

whenever the back-off timer reaches zero. When there are collisions during the transmission or when the transmission fails, the node doubles the value of CW until it reaches the maximum value CW_{max}. Then, the node starts the back-off process again, and retransmits the packet when the back-off is complete. If the maximum transmission failure limit is reached, the retransmission will stop, CW will be reset to the initial value CW_{min}, and the packet will be discarded.

The 802.11 DCF protocol provides two access mechanisms. One is the two-way handshake, i.e., DATA/ACK, and the other is the four-way handshake, i.e., RTS/CTS/DATA /ACK. When the length of DATA packets is long, short frames Request-To-Send (RTS) and Clear-To-Send (CTS) should be used to avoid the possible long collision period of DATA packets. The four-way handshake is shown in Figure 2.1. When the source node senses the channel is idle, it waits for a DIFS period and senses the channel again. If the channel is still idle, the source node transmits an RTS frame to the destination node. All the nodes hearing the RTS frame set their NAVs accordingly. The destination node responds to the RTS frame with a CTS frame after an SIFS (Short Inter-Frame Space) idle period has elapsed. Nodes hearing the CTS frame update their NAVs. Upon successful reception of the CTS, the source node begins to transmit the DATA packet to the destination node. Upon receipt of the correct DATA packet, the destination node waits an SIFS interval and transmits a positive acknowledgment frame (ACK) back to the source node, indicating that the transmission was successful.

2.1.2 Carrier Sensing Range

In the carrier sense mechanism, a node determines the channel is busy when the received signal power exceeds a certain threshold, referred to as carrier sense threshold (CST). Otherwise, the channel is determined idle. It can be seen clearly that the value of CST decides the sensing range and affects both the collision possibility and spatial reuse in MANETs, since a smaller CST means the node can sense the signal in a larger sensing range, and vice versa. The larger the sensing range, the smaller the possibility that a new

transmission attempt interferes with some ongoing transmissions. On the other hand, a larger sensing range implies that more nodes have to defer their transmissions when one node is transmitting, which leads to lower spatial reuse. Usually, the sensing range is larger than the transmission range since the power needed to sense is smaller than that needed to transmit. Figure 2.2 shows both transmission and sensing ranges of a node.

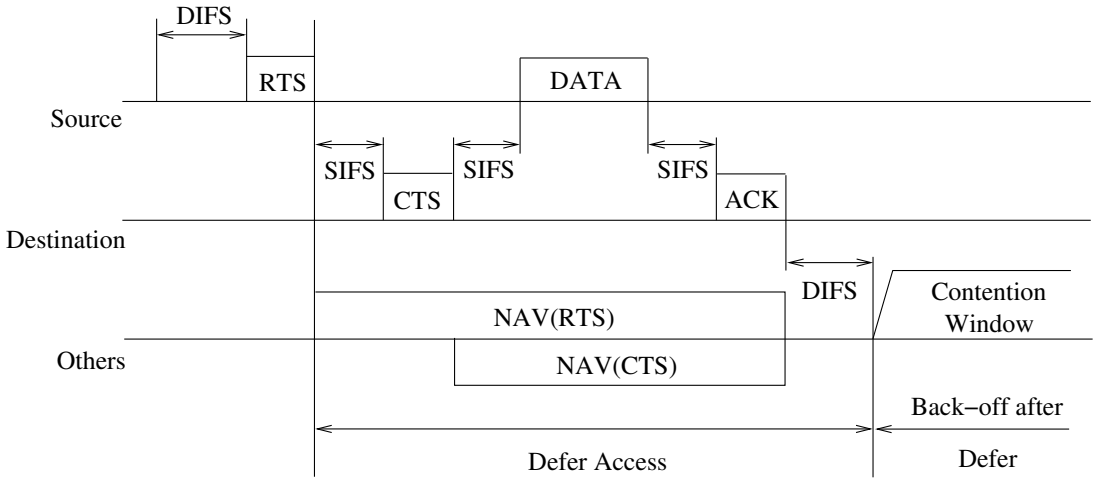

Figure 2.1: RTS/CTS/DATA/ACK Handshake.

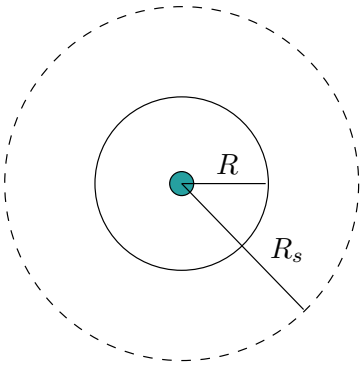

Figure 2.2: Transmission and Sensing Ranges of a Node. (The small and large circles denote the transmission and sensing range, respectively.)

2.1.3 Persistent Probability

In the 802.11 DCF protocol, a node with a new packet to transmit senses the channel. If the channel is idle for a period of time equal to DIFS, the node transmits. The length of DIFS is equal to SIFS plus two time slots. This mechanism reduces the collisions caused by the propagation delay, because there is a small chance that just after a node begins sending, another node will become ready and sense the channel; if the first node's signal has not yet reached the second one, the latter will sense an idle channel and will also begin sending, resulting in a collision. The longer the propagation delay, the larger the possibility of the collision.

Even if the propagation delay is zero, there will still be collisions. If two nodes become ready in the middle of a third node's transmission, both will wait politely until the transmission ends. If they happen to have the same back-off timer, then both will begin transmitting exactly simultaneously, resulting in a collision. DIFS cannot avoid this kind of collisions. To address this problem, some MAC protocols introduce a probability p [50, 57]. When a nodes becomes ready to send, it senses the channel. If it is idle, it transmits with a probability p. With a probability $1-p$, it defers until the next slot. If that slot is also idle, it either transmits or defers again, with probability p and $1-p$. We call p the *persistent probability* in this thesis, since this mechanism is similar to p-persistent CSMA [30]. It is demonstrated that for p-persistent CSMA the throughput of the network increases along with the decrease of p from 1 to 0.01 [48]. However, if p is too small, the delay for each transmission will be very long, which leads to lower spatial reuse.

2.1.4 Back-off Mechanisms

Although BEB is widely used in many contention-based MAC protocols for its simplicity and good performance, it is not a perfect back-off mechanism in fairness and efficiency. In BEB, each node doubles its CW size after every failed transmission, and resets its CW to the minimum value after every successful transmission. Therefore, it might be quite likely that a node that has won the collision and transmitted successfully will capture

the channel again in the following channel contention. The worst case is that one node monopolizes the channel while all other nodes are completely excluded for channel access. On the other hand, BEB becomes inefficient when there are many active nodes and hence aggravates the contention of the channel [5, 64]. Analysis has shown that after reaching its peak, the aggregate throughput decreases along with the input traffic and the number of active nodes.

Because of the drawbacks of BEB, some new back-off mechanisms were proposed [4, 6, 10, 45]. A multiplicative increase and linear decrease (MILD) mechanism is adopted in the MACAW protocol [4] to address the large variation of the contention window size and the unfairness problem of BEB. In MILD, the contention window size is multiplied by 1.5 upon a collision but decreased by 1 step upon a successful transmission, where the step is defined as the transmission time of an RTS frame. MILD performs well when the traffic load is steadily heavy. However, the "linear decrease" sometimes is too conservative, and it degrades the performance when the traffic load is light or the number of active nodes changes sharply [45]. To overcome these problems, the exponential increase exponential decrease (EIED) back-off algorithm has been studied in [45, 58]. In the EIED algorithm, the contention window size is increased and decreased exponentially on every collision and successful transmission, respectively. As a result, EIED is not as conservative as the "linear decrease" of MILD and not as radical as the "reset" of BEB. Realizing that there is a different optimal contention window size for different number of active nodes, many studies focused on adaptive contention window schemes [6, 10]. By collecting observed collision statistics, these schemes estimate the number of currently active nodes and hence calculate a new contention window size to schedule the next transmission. In these schemes, timely and accurate estimate of the number of active stations is a prerequisite for significant performance improvements.

2.1.5 Multiple Handshakes

We can divide the multiple handshakes between a sender and a receiver into two basic categories, i.e., sender-initiated and receiver-initiated. Both the two-way DATA/ACK and four-way RTS/CTS/DATA/ACK handshake of the IEEE 802.11 MAC protocol are sender-initiated. The sender initiates the handshake only when it has packets to send. In the four-way handshake, the exchange of RTS and CTS frames between a sender and a receiver notifies overhearing nodes to defer their access to the shared channel so as to avoid collisions. In the receiver-initiated handshake, a receiver polls its neighbors actively to see if they have packets for itself. For example, MACA-BI (multiple access collision avoidance by invitation) [47] adopts a three-way handshake, i.e., CTS/DATA/ACK, to control the channel access where the CTS frame serves as the polling frame. The three-way handshake has less control overhead than the four-way handshake of the IEEE 802.11 MAC protocol, which explains why MACA-BI outperforms the four-way handshake of the IEEE 802.11 when traffic characteristics are stationary or predictable. However, it does not work well in the dynamic MANET environment because the polled nodes may have no packets for the polling node and the transmission time of polling packets is therefore wasted [28].

Having introduced the basic mechanisms in MAC protocols in MANETs, we investigate a variety of MAC protocols that have been proposed for ad hoc networks, as shown in Table 2.1. These MAC protocols are all sender-initiated protocols, since for generalized ad hoc networks a sender-initiated protocol is more suitable [28]. We investigate their handshake schemes, back-off schemes, and carrier sensing schemes. We also examine the number of channels employed in each MAC protocol. From Table 2.1, we have the following conclusions:

1. Almost all the MAC protocols adopt the RTS/CTS handshake scheme.
2. BEB is widely used as the back-off mechanism.
3. Most of these MAC protocols sense the channel before a transmission starts.
4. Single channel is still the first choice for most MAC protocols.

Protocol	Handshake	Back-off	Carrier Sense	Single/ Multi Channel
Carrier Sense Multiple Access (CSMA) [31]	No.	No.	Yes(n-persistent algorithms).	Single
Medium Access Collision Avoidance (MACA) [29]	RTS/CTS/ DATA	BEB	No.	Single
MACA for Wireless LAN's (MACAW) [4]	RTS/CTS/ DS(Data Sending)/ DATA/ACK	MILD	No(use DS packet).	Single
Floor Acquisition Multiple Access (FAMA) [18]	RTS/CTS/ DATA	Uniformly distributed back-off scheme.	Yes(non-persistent carrier sensing).	Single
802.11 MAC [56]	RTS/CTS/ DATA/ACK	BEB	CSMA-CA	Single
Differentiated Distributed Coordination Function (DDCF) [8]	RTS/CTS/ DATA/ACK	BEB	CSMA-CA	Single
Received-Based AutoRate (RBAR) [26]	RTS/CTS/ DATA	Any.	Yes.	Single
Controlled Access-CDMA (CA-CDMA) [36]	RTS/CTS/ DATA	Any.	Yes.	2 channels
Dual-Busy Tone Multiple Access (DBTMA) [25]	RTS/CTS/ DATA	BEB or MILD	Yes.	2 channels
Bidirectional Multi-Channel MAC (Bi-MCMAC) [32]	RTS/CTS/ DATA/ACK	BEB	Yes.	4 channels
Power Control MAC (PCM) [27]	RTS/CTS/ DATA/ACK	Any.	Yes.	Single

Table 2.1: Comparison of MAC Protocols.

Based on the above conclusions, we assume the MAC protocol used in our analysis to be like this:

1. A source node senses the channel before transmits. When the channel is idle, the node begins its transmission with the persistent probability p.

2. The transmission process uses the RTS/CTS/DATA/ACK handshake scheme. The control packets and data packets are transmitted in a single channel.

3. If the transmission is unsuccessful, the node will back off a period of time $\bar{T}_b$ to retransmit. Three different back-off mechanisms are used for comparison, i.e., BEB, MILD, and EIED, which were described in Section 2.1.4.

Examples of ad hoc MAC protocols close to the above general framework are the RTS/CTS mode of IEEE 802.11 DCF [56] and FAMA [19]. In fact, the schemes of our MAC protocol are similar to most MAC protocols listed in Table 2.1. Therefore, our capacity analysis in Chapter 3 can be generalized to most MAC protocols in Table 2.1.

In summary, this section introduced three basic mechanisms in MAC, i.e., carrier sense, back-off and handshake, then discussed some MAC protocols for back-off and handshake mechanisms. Next, we will present some solutions to the classical hidden terminal and exposed terminal problem in MANETs.

2.2 Hidden Terminal and Exposed Terminal Problems

In MANETs, the hidden terminal problem is the main reason for collisions, and the exposed terminal problem limits the spatial reuse as previously discussed in Section 1.3. Since multi-hop transmissions in MANETs span a large area, and each node may have multiple hidden terminals, therefore the hidden terminal problem is common. This differs from a single wireless LAN, where each node can sense all others' transmissions and requires only one-hop wireless transmissions.

The busy tone signal sent over a separate channel is widely used in many schemes to overcome the hidden terminal problem, or the exposed terminal problem, or both [15, 25, 50]. In the busy tone multiple access (BTMA) scheme [50], a base station broadcasts a busy tone signal to keep the hidden terminals from accessing the channel when it senses a transmission. But the kind of centralized network infrastructure is not available in MANETs. The dual busy tone multiple access (DBTMA) scheme [15, 25] employs the transmit busy tone at the transmitter to prevent the exposed terminals from becoming new receivers, and the receive busy tone at the receiver to prevent the hidden terminals from becoming new transmitters. In this way, the exposed terminals can transmit, and the hidden terminals can reply to RTS requests and receive data.

The floor acquisition multiple access (FAMA) [19] scheme provides another solution to the hidden terminal problem. It uses long CTS frames instead of a busy tone signal to prevent any competing transmitters in the receiver's range from transmitting. To guarantee that there is no collision with an ongoing data transmission, this scheme requires each node that hears the interference to keep silence for a period of one maximum data packet. Clearly, this is inefficient when DATA packets are relatively short.

2.3 Performance Analysis of MAC Protocols

In the previous sections, we have reviewed some representative MAC protocols for MANETs. Especially, we examined the basic mechanism of IEEE 802.11 MAC protocol in Section 2.1. We have shown in Section 1.3 that MAC affects the capacity of MANETs. In order to estimate the capacity of MANETs, it is important to know the upper limit of the throughput of a MAC link. IEEE 802.11 DCF protocol is widely used in MANETs. There have been various papers to model and analyze the saturation throughput of the IEEE 802.11 DCF protocol. In this section, we introduce the existing analysis for IEEE 802.11 DCF, and more generally, for collision avoidance MAC protocols. We will propose our analysis on the basis of them in the next chapter.

2.3.1 Analytical Model of IEEE 802.11 DCF

As mentioned in Section 2.1, IEEE 802.11 DCF is a very popular collision avoidance MAC protocol. It is a random access scheme, based on the carrier sense multiple access with collision avoidance (CSMA/CA) protocol. Retransmission of collided packets is managed according to BEB rules.

In the literature, performance evaluation of 802.11 has been carried out either by means of simulation [14, 54] or by means of analytical models with simplified back-off rule assumptions. In particular, constant or geometrically distributed back-off window has been used in [6, 9, 12] while [7] has considered an exponential back-off limited to two stages (maximum window size equal to twice the minimum size) by employing a two-dimensional Markov chain analysis.

G. Bianchi [5] provided a model that accounts for all the exponential back-off protocol details, and allows to compute the saturation (asymptotic) throughput performance of DCF for both standardized access mechanisms (and also for any combination of the two methods). He defined the system throughput S as the fraction of time the channel is used to successfully transmit payload bits. Let P_{tr} be the probability that there is at least one transmission in the considered slot time. Given n stations contend on the channel, and each transmits with probability τ

$$P_{tr} = 1 - (1 - \tau)^n. \tag{2.1}$$

The probability P_s that a transmission occurring on the channel is successful is given by the probability that exactly one station transmits on the channel, conditioned on the fact that at least one station transmits, i.e.,

$$P_s = \frac{n\tau(1-\tau)^{n-1}}{P_{tr}} = \frac{n\tau(1-\tau)^{n-1}}{1-(1-\tau)^n}. \tag{2.2}$$

Then S can be expressed as the ratio

$$S = \frac{E[\text{payload information transmitted in a slot time}]}{E[\text{length of a slot time}]}. \tag{2.3}$$

Being $E[P]$ the average packet payload size, the average amount of payload information successfully transmitted in a slot time is $P_{tr}P_sE[P]$, since a successful transmission occurs

in a slot time with probability $P_{tr}P_s$. The average length of a slot time is readily obtained considering that, with probability $1 - P_{tr}$, the slot time is empty; with probability $P_{tr}P_s$ it contains a successful transmission, and with probability $P_{tr}(1 - P_s)$ it contains a collision. Hence Equation (2.3) becomes

$$S = \frac{P_s P_{tr} E[P]}{(1 - P_{tr})\sigma + P_{tr} P_s T_s + P_{tr}(1 - P_s) T_c}. \tag{2.4}$$

Here, T_s is the average time the channel is sensed busy (i.e., the slot time lasts) because of a successful transmission, and T_c is the average time the channel is sensed busy by each station during a collision. σ is the duration of an empty slot time. The values $E[P]$, T_s, T_c and σ must be expressed with the same unit. To specifically compute the throughput for a given DCF access mechanism it is now necessary only to specify the corresponding values T_s and T_c.

For basic access mechanism, let

$$H = PHY_{hdr} + MAC_{hdr} \tag{2.5}$$

be the packet header, and δ be the propagation delay. In the basic access,

$$T_s = H + E[P] + SIFS + \delta + ACK + DIFS + \delta, \tag{2.6}$$

$$T_c = H + E[P^*] + DIFS + \delta, \tag{2.7}$$

where $E[P^*]$ is the average length of the longest packet payload involved in a collision.

In the case all packets have the same fixed size, $E[P^*] = E[P] = P$. In the general case, the payload size of each collided packet is an independent random variable P_i. It is thus necessary to assume a suitable probability distribution function $F(\cdot)$ for the packet's payload size. Let P_{max} be the maximum payload size. Taking the conditional expectation on the number k of colliding packets, $E[P^*]$ writes as follows:

$$\begin{aligned} E[P^*] &= E[E[\max(P_1, ..., P_k)|k]] \\ &= \frac{\sum_{k=2}^{n} \binom{n}{k} \tau^k (1-\tau)^{n-k} \int_0^{P_{max}} (1 - F(x)^k) dx}{1 - (1-\tau)^n - n\tau(1-\tau)^{n-1}}. \end{aligned} \tag{2.8}$$

When the probability of three or more packets simultaneously colliding is neglected, Equation (2.8) simplifies to be

$$E[P^*] = \int_0^{P_{max}} (1 - F(x)^2) dx. \tag{2.9}$$

For RTS/CTS access mechanism, collision can occur only on RTS frames, it is:

$$\begin{aligned} T_s &= RTS + SIFS + \delta + CTS + SIFS + \delta + H + \\ &\quad + E[P] + SIFS + \delta + ACK + DIFS + \delta, \end{aligned} \tag{2.10}$$

$$T_c = RTS + DIFS + \delta, \tag{2.11}$$

and the throughput expression depends on the packet size distribution only through its mean.

In summary, G. Bianchi provided an extensive throughput performance evaluation of both access mechanisms of the 802.11 protocol. However, his model is limited for single-hop MANETs. As shown in [28], a multi-hop topology is more suitable to ensure scalability in MANETs, and is the direction of future development. It is meaningful to investigate the performance of the RTS/CTS mechanism with a multi-hop network model, as the potential interference from hidden nodes always exists in multi-hop MANETs.

2.3.2 Analytical Model of Collision Avoidance MAC Protocols

It is very important to investigate the performance of the four-way sender-initiated collision avoidance scheme with a truly multi-hop network model as potential interference from hidden nodes always exists, which is a salient characteristic of multi-hop ad hoc networks. Y. Wang and J. J. Garcia-Luna-Aceves [53] firstly adopt a simple multi-hop network model to derive the saturation throughput of a sender-initiated collision avoidance scheme, in which nodes are randomly placed on a plane according to two-dimensional Poisson distribution with density λ. Varying λ has the effect of changing the congestion level within a region as well as the number of hidden terminals. The adoption of a Poisson distribution is due to its tractability for analysis and ability to model multi-hop networks. In this model, it is also assumed that each node is ready to transmit independently in each time

slot with probability p, where p is a protocol-dependent parameter. This model was first used by Takagi and Kleinrock [46] to derive the optimum transmission range of a node in a multi-hop wireless network, and was used subsequently by Wu and Varshney [59] to derive the throughput of non-persistent CSMA and some variants of busy tone multiple access (BTMA) protocols [50]. Then they assume that both carrier sensing and collision avoidance work perfectly, that is, that nodes can accurately sense the channel busy or idle, and that the RTS/CTS mechanism can avoid the transmission of data packets that collide with other packets at the receivers. The latter assumption can be called perfect collision avoidance and has been shown to be doable in the floor acquisition multiple access (FAMA) protocol [21].

With the model and assumptions, they present the analysis of the basic four-way sender-initiated collision avoidance scheme. They use a Markov chain model for the channel around a node to get the equation

$$p' = \frac{pT_{idle}}{T_{idle} + P_{il}T_{long} + P_{is1}T_{short1} + P_{is2}T_{short2}}. \tag{2.12}$$

In the above equation, p is the probability that a node is ready to transmit, and p' is the probability that a node does transmit in a time slot.

If the length of each time slot is denoted by τ, which represents the time required for all the nodes within the transmission range to know the event that occurred τ seconds ago, and the transmission times of RTS, CTS, DATA, and ACK frames are normalized with regard to τ and are denoted by l_{rts}, l_{cts}, l_{data}, and l_{ack}, then the duration of the idle state $T_{idle} = \tau$. The busy time of the whole handshake

$$\begin{aligned} T_{long} &= l_{rts} + \tau + l_{cts} + \tau + l_{data} + \tau + l_{ack} + \tau \\ &= l_{rts} + l_{cts} + l_{data} + l_{ack} + 4\tau. \end{aligned} \tag{2.13}$$

The busy time that when multiple nodes around the channel transmit RTS frames during the same time slot and their transmissions collide is $T_{short1} = l_{rts} + \tau$. The busy time when the channel is in effect busy, i.e., unusable for all the nodes, is

$$T_{short2} = l_{rts} + \tau + l_{cts} + \tau = l_{rts} + l_{cts} + 2\tau. \tag{2.14}$$

The transition probability from *idle* to *idle* P_{ii} is given by

$$P_{ii} = \sum_{i=0}^{\infty}(1-p')^i \frac{M^i}{i!}e^{-M} = e^{-p'M}. \tag{2.15}$$

Let p_s denote the probability that a node begins a successful four-way handshake at each slot. We can then calculate the transition probability from *idle* to *long* P_{il} as follows:

$$P_{ii} = \sum_{i=1}^{\infty} ip_s(1-p')^{i-1} \frac{M^i}{i!}e^{-M} = e^{-p'M}. \tag{2.16}$$

The transition probability from *idle* to *short1* P_{is1} is:

$$\begin{aligned} P_{is1} &= \sum_{i=2}^{\infty}[1-(1-p')^i - ip'(1-p')^{i-1}]\frac{M^i}{i!}e^{-M} \\ &= 1-(1+Mp')e^{-p'M}. \end{aligned} \tag{2.17}$$

Thus, the transition probability from *idle* to *short2* P_{is2} is equal to $1 - P_{ii} - P_{il} - P_{is1}$. In Equation (2.12), p_s is an unknown variant.

The authors use another model of the states of a node x by a three-state Markov chain. Let π_s, π_w, π_f denote the steady-state probabilities of states *succeed*, *wait* and *fail* respectively. Then the throughput Th is:

$$\begin{aligned} Th &= \frac{\pi_s l_{data}}{\pi_w T_w + \pi_s T_s + \pi_f T_f} \\ &= l_{data}\pi_s[\tau\pi_w + (l_{rts} + l_{cts} + 2\tau)(1-\pi_w-\pi_s) + \\ &\quad +(l_{rts} + l_{cts} + l_{data} + l_{ack} + 4\tau)\pi_s]^{-1}. \end{aligned} \tag{2.18}$$

Here π_s is just the previous unknown quantity p_s in Equation (2.12).

$$\pi_s = \pi_w P_{ws} = \frac{P_{ws}}{2-(1-p')e^{-p'N}}, \tag{2.19}$$

where P_{ws} is the transition probability from *wait* to *succeed*,

$$P_{ws} = 2p'(1-p')e^{-p'N}\int_0^1 re^{-p'N[1-2q(r/2)/\pi](2l_{rts}+1)}dr, \tag{2.20}$$

and

$$q(t) = \arccos(t) - t\sqrt{1-t^2}. \tag{2.21}$$

The results show that the four-way handshake MAC protocols outperform CSMA protocols, even when the overhead of RTS/CTS exchange is rather high, thus showing the importance of correct collision avoidance in random access protocols. More importantly, it is shown that the overall performance of the sender-initiated collision avoidance scheme degrades rather rapidly when the number of competing nodes allowed within a region increases, in contrast to the case of fully-connected networks and networks with limited hidden terminals reported in the literature [5, 10, 11], where throughput remains almost the same for a large number of nodes. The significance of the analysis is that the scalability problem of contention-based collision avoidance MAC protocols looms much earlier than people might expect. Simulation experiments with the IEEE 802.11 MAC protocol validate these observations and show that the IEEE 802.11 MAC protocol can suffer severe degradation in throughput due to its inability to avoid collisions between data packets and other packets even when the number of competing nodes in a region is small. However, when the number of competing nodes in a region increases, the performance gap is smaller as perfect collision avoidance protocols also begins to suffer from exceedingly long waiting time.

As introduced above, Wang and Garcia presented a successful analysis to the collision avoidance protocols in MANETs. However, there exist some problems in their work. First, the back-off mechanism used in the model is too simple, and the authors did not compare the effect of different back-off mechanisms. Second, in their analysis, they consider the hidden terminal problem in the transmission range of nodes, but according to our introduction in Section 1.3, the hidden terminal problem exists not only in transmission range, but also in sensing range of nodes. Third, to calculate the throughput from their formula, we must know the node density, which is difficult to obtain in a practical MANET. Furthermore, the vulnerable period of RTS in the analysis is inaccurate which will be shown in Section 3.3.1. We will modify this model and improve these problems to perform our capacity analysis in Chapter 3.

2.4 Capacity Analysis for MANETs

In the last decade, much research [22, 23, 24, 33, 40, 67] has been carried out to study the capacity of MANETs. Currently, the "capacity of MANETs" has been given several different definitions with respect to "throughput capacity"[24], "transport capacity"[24], "throughput per node"[33], "bits-per-Joule capacity"[40] and "number of sessions that can be supported in the network"[67], etc. In each definition, one or more factors affecting the capacity are considered, such as the number of nodes [24, 33], transmission range [33], energy of nodes [40], number of hops [67], etc.

Gupta and Kumar [24] presented the most significant results of the capacity of wireless networks, which is a good start to study the capacity of MANETs. They proposed two definitions of capacity for wireless networks as they consider two types of networks. One is *Random Networks*, where the nodes and their destinations are randomly chosen. The other one is *Arbitrary Networks*, where the node locations, destinations of sources, and traffic demands are all arbitrary so that they can be configured to be optimal. For both types of networks, two types of wireless transmission reception models are used, i.e., protocol and physical models. In the protocol model, a successful transmission is determined based on the ratio of the distances. In the physical model, a transmission is successful when the signal-to-interference-and-noise ratio (SINR) is greater than a threshold. For a random network, *throughput capacity* is proposed to describe the capacity of the network, as defined below.

Definition 1 The Throughput Capacity of Random Networks [24]: In a random wireless network, where the locations of nodes and their destinations are randomly chosen, given n homogeneous fixed nodes employing the same transmission range or power, a throughput of $C(n)$ bits per second for each node is *feasible* if there is a spatial and temporal scheme for scheduling transmissions, such that by operating the network in a

multi-hop fashion and buffering at intermediate nodes when awaiting transmission, every node can send $C(n)$ bits per second on average to its chosen destination node. Therefore, the *throughput capacity* of the class of random networks is of order $\Theta(f(n))$ bits per second if there are deterministic constants $c > 0$ and $c' < +\infty$ such that

$$\lim_{n\to\infty} Prob(C(n) = cf(n) \ is\ feasible) = 1, \tag{2.22}$$

$$\liminf_{n\to\infty} Prob(C(n) = c'f(n) \ is\ feasible) < 1, \tag{2.23}$$

where $\Theta(f(n))$ is referred to Knuth's notation.

This definition counts the number of nodes as a factor affecting the capacity. In order to derive the *throughput capacity*, the authors constructed a scheduling and routing scheme. The scheduling scheme for transmitting packets is that if a node has c_1 interfering neighbors, in every $(1 + c_1)$ slots, each node gets one slot in which to transmit, and such that all transmissions are successfully received within the transmission range of their transmitters; no collision occurs. The routing scheme utilizes a Voronoi tessellation [38] to route traffic efficiently through the random graph so that no node is overloaded. Assuming each node is capable of transmitting at W bits per second, the order of the *throughput capacity* obtainable by each node for a randomly chosen destination is calculated by

$$C(n) = \Theta(\frac{W}{\sqrt{n \log n}}) \qquad \text{bits per second} \tag{2.24}$$

for the protocol model. For the physical model, a throughput of

$$C(n) = \frac{cW}{\sqrt{n \log n}} \qquad \text{bits per second} \tag{2.25}$$

is feasible, while

$$C(n) = \frac{c'W}{\sqrt{n}} \qquad \text{bits per second} \tag{2.26}$$

is not, for appropriate c and c', both with probability approaching one as $n \to \infty$.

From the results in Equation (2.24) and (2.25), we note that the capacity of a random network decreases when the number of nodes increases. The same implication exists for an arbitrary network. In an arbitrary network, in order to place the nodes appropriately, the distance between the source and destination of a bit becomes important, so the *bit-meter* is introduced. The network transports one *bit-meter* when one bit has been transported a distance of one meter toward the destination. On basis of this, *transport capacity* is defined in the following to describe the capacity of the network.

Definition 2 The Transport Capacity of Arbitrary Networks [24]: In an arbitrary wireless network, given n inhomogeneous fixed nodes, if the bits transmitted from the source node i to its destination is b_i, the distance between the source node i and its destination is d_i, the sum of products of bits and the distances over which they are carried is defined as a network's *transport capacity*, i.e.,

$$C(n) = \sum_{i=1}^{n} b_i d_i \qquad \text{bit-meters per second.} \tag{2.27}$$

This definition considers the number of nodes, the bits transmitted, and the transmission distance. In the transmission, no scheduling mechanism is used to avoid collisions. Instead, the destination node uses a comparison mechanism to restrain the interference. Suppose node i transmits over the channel to a node j, then this transmission is successfully received by node if

$$|k - j| \geq (1+ \triangle)|i - j| \tag{2.28}$$

for every other node k simultaneously transmitting over the same channel. The quantity $\triangle > 0$ models situations where a guard zone is specified by the protocol to prevent a neighboring node from transmitting on the same channel at the same time. If n inhomogeneous fixed nodes are optimally placed in a disk of area A, each capable of transmitting at W bits per second, traffic patterns are optimally assigned, and each transmission's range is optimally

chosen, the *transport capacity* of an arbitrary network under the protocol model is

$$C(n) = \Theta(W\sqrt{An}) \qquad \text{bit-meters per second.} \tag{2.29}$$

Here "optimally" means that we choose an appropriate location, transmission range, and traffic pattern for each node so that each transmitter can transmit to its nearest receiver without interference from any other transmitter-receiver pair. For the physical model,

$$C(n) = cW\sqrt{An} \qquad \text{bit-meters per second} \tag{2.30}$$

is feasible, while

$$C(n) = c'Wn^{\frac{\alpha-1}{\alpha}}\sqrt{A} \qquad \text{bit-meters per second} \tag{2.31}$$

is not, for appropriate c and c'. α is the attenuation index which means that the signal power decays with distance r as $\frac{1}{r^{\alpha}}$.

From the results in Equation (2.29) and (2.30), we note that the area size, node locations, the number of nodes and the bandwidth of a node are considered. The authors presented rigorous theoretical analysis to derive the lower and upper bounds of network capacity. From the analytical results, it follows that the throughput capacity per node reduces significantly when the node density increases. The analytical approach in [24] has significantly driven the progress in capacity research of MANETs. However, their work lacks practical applicability because the networking protocols have not been fully captured by their analysis. For example, in MAC layer, an ideal schedule for the transmissions is assumed in the protocol model for random networks, but the basic components of MAC, i.e., carrier sense, handshake, and back-off mechanisms, which have effects on the network capacity, are not considered in the analysis. Moreover, the nodes are assumed fixed, which does not match the mobility characteristic of MANETs.

Grossglauser and Tse [23] modified the model in [24] and included mobility to the capacity analysis. They proposed a scheme that increases the network capacity of MANETs by utilizing the node mobility. When a node needs to send packets to another node, it will not send until the destination node is close to the source node. Thus, via the node mobility, a node only communicates with its nearby nodes. By allowing for unbounded delay and

using only one-hop relaying but taking advantage of the mobility, they showed an $O(n)$ throughput for an MANET. The limitation of this scheme is obvious: The transmission delay may become large and the required buffer for a node may be infinite.

Gastpar and Vetterli [22] worked on the case of relay capacity while Gupta and Kumar considered only the point-to-point case. They considered the same physical model of a wireless network that Gupta and Kumar used, but under a different traffic pattern. i.e., relay traffic pattern. The key result is that the capacity of the wireless network with n nodes under the relay traffic pattern behaves like $\log n$ bps.

Li et al. [33] extend Gastpar and Gupta's work [22, 24] by further considering the effects of different traffic patterns on the scalability of per node capacity. Their analysis is based on scaling relationships: load increases with the number of nodes, load also increases with the distance over which each node wishes to communicate, and total *one-hop capacity* increases with the physical area covered by a network. The *one-hop capacity* is similar in concept to the bit-meters per second unit proposed in [24], as defined in the following.

Definition 3 One-hop Capacity [33]: In an n-node MANET, assume each node originates packets at a rate of C. Further, assume the traffic pattern in the network has an expected physical path length of L from the source to the destination. This means that the minimum number of hops required to deliver a packet is $\frac{L}{R}$ where R is the fixed radio transmission range. Hence the total *one-hop capacity* in the network required to send and forward packets λ obeys

$$\lambda > nC\frac{L}{R}. \tag{2.32}$$

The total *one-hop capacity* of the network is determined by the amount of spatial reuse possible in the network. Given constant radio range, spatial reuse is proportional to the physical area of the network. Clearly, the total *one-hop capacity* of the network should be proportional to the area. Assuming that the node density δ is uniform, the physical

area of the network, A, is related to the total number of nodes by $A = \frac{n}{\delta}$. Then, the total *one-hop capacity* of the network, λ, can be written as

$$\lambda = kA = \frac{kn}{\delta} \qquad \text{for some constant } k. \tag{2.33}$$

Combining Equation (2.32) and (2.33), we have

$$\frac{kn}{\delta} > \frac{nCL}{R}. \tag{2.34}$$

Therefore, given the *one-hop capacity* defined in Definition 3, from Equation (2.34) we can obtain the capacity of each node consequently, which is defined as the *packet rate per node* [33] in the following.

Definition 4 Packet Rate per Node [33]: Assume each node originates packets at a rate of C. If R is the fixed radio transmission range, L is the physical path length from the source to the destination, then the *capacity* available to each node, C, is bounded by

$$C < \frac{kR}{\delta L} = \frac{\lambda/n}{L/R}. \tag{2.35}$$

In this definition, the transmission range, path length, and node density are considered. When the node density and transmission range are constants, the path length has a great impact on the capacity. The path length is determined by the traffic pattern. The most common traffic pattern used in simulations of ad hoc networks has been random traffic: each source node initiates packets to randomly chosen destinations in the network. The authors derived the path length L for such traffic. First, they showed that the probability of a node communicating with another node at distance x as

$$p(x) = \frac{x}{\int_0^{\sqrt{A}} t dt}. \tag{2.36}$$

Therefore, the expected path length for a random traffic pattern is

$$L = \int_0^{\sqrt{A}} x p(x) dx = \frac{2\sqrt{A}}{3}. \tag{2.37}$$

Thus we find that L is only related with A. When the node density is known, the physical area of the network, A, is proportional to the number of nodes, n. Therefore, the capacity available to each individual node, C is $O(\frac{1}{\sqrt{n}})$. Other than the random traffic pattern, the authors also investigated a number of concrete traffic patterns that might allow the per node capacity to scale well with the size of the network. They showed that the less local the traffic pattern, the faster per node capacity degrades with network size.

After analyzing the capacity under different traffic patterns, the authors argued that the key factor deciding whether large ad hoc networks are feasible is the locality of traffic. This result stands true no matter which MAC protocol is in use, since the proof did not consider any mechanisms in MAC layer. Another contribution of Li et al.'s work is the practical analysis of scalability based on IEEE 802.11 networks using the *ns* [17] simulator. Under the four-way RTS/CTS/DATA/ACK handshake mode, they presented the disadvantage of BEB back-off mechanism in 802.11 MAC protocol for MANETs. They also analyzed the capacity of specific topologies, i.e. chain and lattice, by simulation. However, they did not propose a theoretical model for the effects of MAC on the capacity which can match the simulation results. On the other hand, in their analysis of chain topologies, only one source at the end generates traffic and other nodes forward it. This scenario is different from the traffic pattern in MANETs where user nodes are assumed to be equally active.

All the definitions above did not consider the delay in MANETs, or they focused on MANETs carrying delay-tolerant traffic. Actually, the supported services in MANETs are not only delay-tolerant, such as FTP (File Transfer Protocol) and E-mail, but also delay-sensitive real-time applications, such as voice chat. To address the capacity analysis for an MANET supporting delay-sensitive traffic, J. Zhang and W. Seah gave a definition of capacity in [67] using the *number of sessions* supported in the network.

Definition 5 Number of Sessions [67]: Given the topology in an MANET, assume packets are transmitted one hop in each time slot. BW_{node} is the bandwidth of the channel,

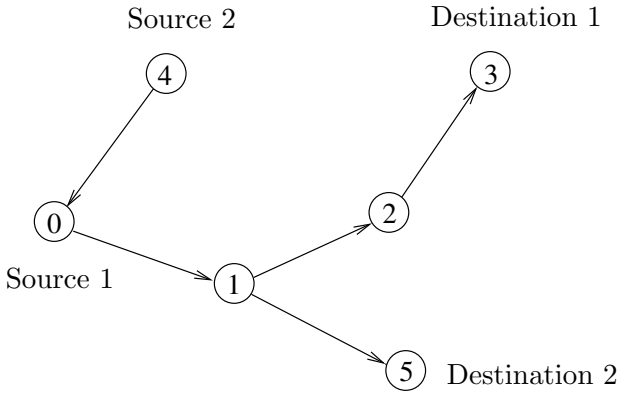

Path 1: $0 \rightarrow 1 \rightarrow 2 \rightarrow 3$	
Hop Count	Sessions
One-hop	$0 \rightarrow 1, 1 \rightarrow 2, 2 \rightarrow 3$
Two-hop	$0 \rightarrow 1 \rightarrow 2, 1 \rightarrow 2 \rightarrow 3$
Three-hop	$0 \rightarrow 1 \rightarrow 2 \rightarrow 3$

Figure 2.3: Paths and Sessions.

and BW_{packet} is the bandwidth needed by a packet transmission, so $\lfloor BW_{node}/BW_{packet} \rfloor$ is the number of one-hop sessions that the channel can support. If the sum of hop counts of shortest paths for all the possible communications is denoted by HC, and the number of source-destination pairs is denoted by N_p, then the average hop count $AHC = HC/N_p$. Assuming D_E is the end-to-end delay constraint (measured by hops), D_E/AHC is the delay per hop. If a session comprises one hop or several sequential hops without considering whether nodes on it are source, destination, or intermediate nodes (Figure 2.3), the *capacity* of this MANET is defined as the number of one-hop sessions that can be supported in the network under end-to-end delay constraints:

$$C = \min \left[\left\lfloor \frac{BW_{node}}{BW_{packet}} \right\rfloor, \frac{D_E}{AHC} \right], \tag{2.38}$$

where $\lfloor x \rfloor$ denotes the largest integer that does not exceed x.

In this definition, the number of hops, bandwidth of the channel, bandwidth needed by a packet transmission and the end-to-end delay constraint are considered. In their analysis, a simple transmission rule is adopted to avoid the interference during the transmissions. As shown in Figure 2.4, when node 1 is transmitting, the node 4 can transmit simultaneously while node 2 and node 3 cannot due to interference. With this transmission rule the authors presented that the average hop count is

$$AHC = \frac{\sum_{i \in B(n,n)} i - n}{n^2 - n - n_0}. \tag{2.39}$$

In Equation (2.39), $B(n, n)$ is a matrix of $\{b_{ij}\}$ where b_{ij} denotes the number of hops between node i and node j. If the number of hops exceeds the end-to-end delay constraint, then $b_{ij} = 0$. n_0 is the number of the items with value 0 in the matrix $B(n, n)$.

With these factors, the maximum number of one-hop sessions that share the same channel is evaluated. From the definition and analysis, the authors proposed that the

capacity of MANETs is restricted by the bandwidth of channels as well as the end-to-end delay constraint. When the end-to-end delay constraint is small, it limits the number of sessions sharing the same channel. By increasing the end-to-end delay constraint, the network capacity would be limited mainly by the bandwidth of the channel. Therefore, the capacity cannot increase unlimitedly. Meanwhile, Equation (2.38) shows that the smaller the average hop count of the flows, the more simultaneous one-hop sessions, and thus the higher capacity of the network. The limitation of Zhang and Seah's work is that they did not consider the handshake and back-off mechanisms in MAC layer, and the delay in nodes due to contention for the channel access, which are not negligible in real MANETs.

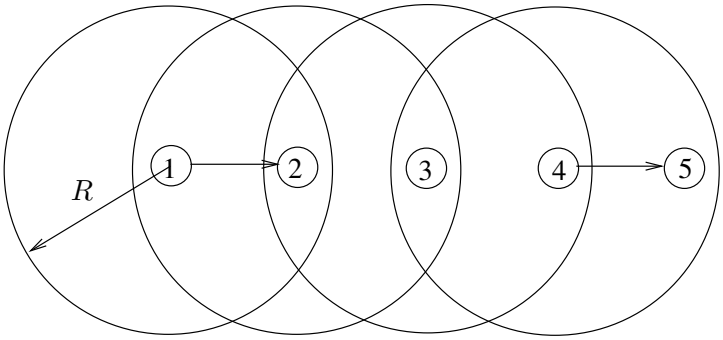

Figure 2.4: Transmission Property. (R is the transmission range of each node.)

So far, the MANETs studied in the above literature have no constraints on the node energies. However, due to the mobility and portable characteristic of nodes in MANETs, energy is always a limiting resource and thus affects the capacity. To address this issue, V. Rodoplu and T. Meng [40] developed a framework to evaluate the capacity of MANETs in which the energy supply of the nodes is the primary resource constraint. They use the "bits-per-Joule capacity" to measure the capacity of MANETs, and define the *bits-per-Joule capacity* as the maximum number of bits that can be delivered per Joule of energy in the network.

Definition 6 Bits-per-Joule Capacity [40]: If the maximum number of bits that the

network can deliver is denoted as N_b, the sum of the nodes' energies is denoted as J, then the *bits-per-Joule capacity* of the network is

$$C = \frac{N_b}{J} \qquad \text{bits per Joule.} \tag{2.40}$$

In Equation (2.40), the maximum number of delivered bits and the energy of nodes are considered. Clearly, N_b is needed to calculate the capacity. In order to derive N_b, three traffic models are studied. The "traffic model" means the specification of the set of source-destination node pairs that have a positive demand $d^{(m,n)}$ which is referred to as the amount of traffic transmitted end-to-end from m to n in the node set $\aleph$. The one-to-one traffic model is that every node generates a traffic demand for exactly one other randomly chosen node. Under this model, N_b is taken to be

$$N_b = \max \sum_{m \in \aleph} \sum_{n \in \aleph} d^{(m,n)} \tag{2.41}$$

The many-to-one traffic model is that every node generates a traffic demand for a single destination node (taken as node 1) for the entire network. N_b under this model is taken to be

$$N_b = \max \min_{m \in \aleph\{1\}} d^{(m,1)} \tag{2.42}$$

The one-to-many traffic model is that a single source node (taken to be node 1) generates traffic demands for all the other nodes in the network. N_b under this model is taken to be

$$N_b = \max \min_{m \in \aleph\{1\}} d^{(1,n)} \tag{2.43}$$

Using Definition 6 and N_b in Equation (2.41)-(2.43), Rodoplu and Meng presented simulations for different traffic models and demonstrated that for the one-to-one traffic model, the bits-per-Joule capacity grows with the number of nodes. However, by assuming a interference-free transmission process, their work ignored the interference of nodes, and thus did not consider the effect of MAC in transmissions, which is an important issue as introduced in Section 1.3.

In summary, the *capacity of MANETs* has been investigated in such different ways:

1. *Throughput Capacity* [24]: the number of bits per second obtainable by each node for a randomly chosen destination.

2. *Transport Capacity* [24]: the bit-meter product that can be transported by the network per second.

3. *Packet Rate per Node* [33]: the maximum number of packets per second for each node.

4. *Number of Sessions* [67]: the maximum number of sessions that can be supported in the network under end-to-end delay constraints.

5. *Bits-per-Joule Capacity* [40]: the maximum number of bits that the network can deliver per Joule of energy.

However, these existing analyses are not sufficient to measure the capacity of MANETs, since some important issues, including the effects of MAC layer protocols on the capacity, have not been considered or fully considered in these analyses. For example, the effects of carrier sense, handshake and back-off mechanisms in MAC protocols are not involved in most of these analyses. In [33], the disadvantage of BEB back-off mechanism is presented through simulation, but the authors did not give an analytical model to explain it. We know that MAC protocols have effects on the capacity of MANETs as shown in Section 1.3, and we have presented the basic mechanisms of MAC in Section 2.1. Then, in the next chapter, we will propose an analytical model to evaluate the effects of these mechanisms on the capacity of MANETs.

Chapter 3

Effects of MAC Protocols on the Capacity of MANETs

In this chapter, we analyze the effects of MAC protocols on the capacity of MANETs. In order to perform our analysis, we propose our definition of MANET capacity, which is the throughput of channel based on the persistent probability, average back-off time and sensing range. Then, we present the models used in our analysis, i.e., topology model, channel state model, and node state model. After that, we perform our analysis and derive the close form of the capacity of MANETs. At last, we give the algorithm which is to be used for the simulation in Chapter 4.

3.1 Definition of Capacity in MANETs

In this section, we will propose the definition of capacity in MANETs. Before that, we present some useful results on Markov process.

3.1.1 Preliminaries

Definition 7 If a stochastic process $\{X(t), t \in (0, \infty)\}$ with state space $S = \{s_0, s_1, s_2, ...\}$ has the property that there exist time points at which the process restarts itself, this process is called a *regenerative process*. In other words, for a regenerative process, there exists a time T_r with probability one, such that the continuation of the process beyond T_r is a probabilistic replica of the whole process starting at zero. Define the *limiting probability* P_{s_j} as

$$P_{s_j} = \lim_{t \to \infty} P\{X(t) = s_j\}, \qquad \text{for all } s_j \in S. \tag{3.1}$$

Referring to the time between two regeneration points as a circle, the limiting probability P_{s_j} can be computed as given in the following theorem [41].

Theorem 1 If T_r has an absolutely continuous component (that is, it has a density on some interval), and $E(T_r) < \infty$, then

$$P_{s_j} = \frac{E(T_{s_j})}{E(T)}, \qquad \text{for all } s_j \in S, \tag{3.2}$$

where T_{s_j} is the amount of time in state s_j during one cycle, and T is the time of one cycle.

Definition 8 If a stochastic process which makes transitions from state to state in accordance with a Markov chain, and if the process is also a regenerative process, the stochastic process is called a *Markov regenerative process*.

For Markov regenerative processes, the limiting probability P_{s_j} can be computed as follows [41].

Theorem 2 Let Q_{s_j} be the steady-state probability for state s_j (Q_{s_j} equals the long run proportion of transitions which are into state s_j), T_{s_j} be the mean time spent in state s_j per transition, and P_{s_j} be the limiting probability (P_{s_j} equals the long run probability that the process is in state s_j). If the Markov chain is positive recurrent and irreducible, then

$$P_{s_j} = \frac{Q_{s_j} T_{s_j}}{\sum_{s_i} Q_{s_i} T_{s_i}}, \tag{3.3}$$

where s_i means any states in the state space.

Next, we use this theorem to define the capacity of MANETs.

3.1.2 Definition of Capacity

In the previous literature, the network capacity is widely measured by throughput [3, 5, 24, 33, 37, 53, 59], i.e., how many data bits can be transmitted during a period of time. This is an intuitive metric of the maximum data traffic load that a network can support. However, in order to evaluate the effects of MAC on the capacity in an MANET, we want to take the fraction of time in which the node is engaged in the successful transmission of data packets into account. In the estimation of the fraction part, three basic mechanisms in MAC protocols are involved, i.e., handshake, carrier sense and back-off, which have been illustrated in Section 2.1. Since the four-way RTS/CTS/DATA/ACK handshake is widely adopted in MANETs, we assume such a handshake mechanism in this thesis. To evaluate the effects of carrier sense and back-off mechanisms, we introduce three parameters, i.e., persistent probability, sensing range, and average back-off time, as shown in Table 3.1. Therefore, we can define the capacity of MANETs in the following.

Definition 9 Capacity of MANETs: In MANETs, we assume that the bandwidth of channel is denoted by B_w. All the nodes use the same sensing range of radius R_s and the

same persistent probability p. The average back-off time of each node during a transmission is denoted by $\bar{T}_b$. During the transmission, we assume that each node has three states: a successful transmission state *success*, a wait state *wait*, and a failed transmission state *failure*. We use s_i (i=s, w, f, respectively) to denote these states. For a node with persistent probability p, sensing range R_s, and back-off time $\bar{T}_b$, let $Q_{s_i}(p, R_s, \bar{T}_b)$ be the steady-state probability for state s_i of the node, T_{DATA} be the data transmission time, $T_{s_i}(p, R_s, \bar{T}_b)$ be the time which the node spends on state s_i, then from Equation (3.3) the *capacity of MANETs* is equal to the channel bandwidth multiplying the limiting probability that the node is transmitting data and thus can be denoted by

$$C(p, R_s, \bar{T}_b) = B_w \frac{Q_{s_s}(p, R_s, \bar{T}_b) T_{DATA}}{\sum_{s_i} Q_{s_i}(p, R_s, \bar{T}_b) T_{s_i}(p, R_s, \bar{T}_b)}. \tag{3.4}$$

This definition is distinguished from other definitions reviewed in Section 2.4 by considering both the channel bandwidth and the MAC mechanisms. In Equation (3.4), carrier sense, represented by p and R_s, and back-off, represented by $\bar{T}_b$, are involved. Therefore, through changing these values, we can evaluate the effects of MAC on the capacity of MANETs from Equation (3.4). Besides the three parameters, the transmission range of node, number of neighbors, and transmission time of frames are also considered in the derivation of Q_{s_i} and T_{s_i}, which will be shown in Section 3.3.

To estimate C from Equation (3.4), we need to obtain B_w, T_{DATA}, Q_{s_i} and T_{s_i}, respectively. In this thesis, we assume B_w and T_{DATA} are known, since the channel bandwidth is determined by the properties of the channel, and the data transmission time is determined by the data packet size, beyond the control of MAC. Thus, our work focuses on Q_{s_i} and T_{s_i}. We will use three analytical models which are proposed in Section 3.2 to derive Q_{s_i} and T_{s_i}. Shown in Table 3.2 are the parameters used in these models. In these parameters, T_{RTS}, T_{CTS}, T_{DATA} and T_{ACK} are determined by the size of the frames; τ is a preset

Symbol	Description
p	Persistent probability.
R_s	Sensing range of each node.
$\bar{T}_b$	Average back-off time.

Table 3.1: Parameters of MAC Mechanisms.

Symbol	Description
T_{RTS}	Transmission time of an RTS frame.
T_{CTS}	Transmission time of a CTS frame.
T_{DATA}	Transmission time of DATA frames.
T_{ACK}	Transmission time of an ACK frame.
τ	Length of each time slot.
$\bar{k}$	Average number of neighbors within the sensing range of each node.
R_t	Transmission range of each node.

Table 3.2: Parameters of Our Models.

parameter; $\bar{k}$ is determined by the node distribution; R_t is determined by the transmission power and radio propagation properties (i.e., attenuation). Since all of the parameters are determined by the factors not related to p, R_s and $\bar{T}_b$, they can be considered as known values in our analysis.

We assume that the parameters in Table 3.1 and 3.2 are known. Then, based on our models in Section 3.2, we will derive the functions defined in Table 3.3. As we show in Table 3.3, A, $B(r)$, $E(r)$ and $I(r)$ are the symbols to denote areas and area sizes, where (r) means that the area size is a function of r. $\bar{m}$, $\bar{N}$, $\bar{N_A}$ and $\bar{M}$ denote the average number of nodes in different range of areas. r is the distance between a transmitter and a

Symbol	Description
A	Annulus between two concentric circles of radii R_s and $(R_s + R_t)$.
$B(r)$	Exclusive area which is the part of sensing area of node j but not covered by the sensing range of node i.
$E(r)$	Intersection of the sensing areas of node i and j.
$I(r)$	Intersection area of the sensing area of node i and transmission area of node j.
$\bar{m}$	Average number of collisions for each transmission.
$\bar{N}$	Average number of nodes within the sensing range of each node.
$\bar{N_A}$	Average number of nodes within the region A.
$\bar{M}$	Average number of nodes within the transmission range of each node.
r	Distance between a transmitter and a receiver.
$f(r)$	Probability density function of r.
p_i	Limiting probability that a channel is idle.
p_t	Transmission probability.
P_{ii}	Transition probability from *idle* to *idle* in channel state model.
P_{is}	Transition probability from *idle* to *busy1-success* in channel state model.
P_{if}	Transition probability from *idle* to *busy2-failure* in channel state model.
P_{is1}	Probability that there is at least one successful transmission in node i's sensing area.
P_{is2}	Probability that there is at least one successful reception in node i's sensing area.
P_1	Probability that node i transmits in a slot.
P_2	Probability that node j and all the other nodes except node i within R_s of node i does not transmit in a slot.
$P_3(r)$	Probability that none of the nodes in $E(r)$ transmits for $(T_{RTS} + \tau)$ time.
P_I	Probability that any node in A initiates a successful four-way handshake to a node in $I(r)$.
P_{ww}	Transition probability from *wait* to *wait* in node state model.
P_{ws}	Transition probability from *wait* to *success* in node state model.

(To be continued.)

(Continued.)

Symbol	Description
P_{wf}	Transition probability from *wait* to *failure* in node state model.
π_i	Steady-state probability of *idle* state of channel.
π_{bs}	Steady-state probability of *busy1-success* state of channel.
π_{bf}	Steady-state probability of *busy2-failure* state of channel.
π_w	Steady-state probability of *wait* state of node.
π_s	Steady-state probability of *success* state of node.
π_f	Steady-state probability of *failure* state of node.
T_i	Duration time of *idle* state of channel.
T_{bs}	Duration time of *busy1-success* state of channel.
T_{bf}	Duration time of *busy2-failure* state of channel.
T_w	Duration time of *wait* state of node.
T_s	Duration time of *success* state of node.
T_f	Duration time of *failure* state of node.
$\bar{T_d}$	Average defering time.

Table 3.3: Variables and Functions in Our Analysis.

receiver. $f(r)$ is the probability density function of r. p_i is the limiting probability that a channel is sensed idle. p_t is the transmission probability. P_{ii}, P_{is} and P_{if} are the transition probabilities of channel states. P_{is1} and P_{is2} are the two parts in calculating P_{is}. P_{ww}, P_{ws} and P_{wf} are the transition probabilities of node states. π_i, π_{bs} and π_{bf} are the steady-state probabilities of the channel. π_w, π_s and π_f are the steady-state probabilities of the node. T_i, T_{bs} and T_{bf} are the duration time of channel states. T_w, T_s and T_f are the duration time of node states. The relationships between these variables in our derivation are shown in Figure 3.1 and 3.2.

After deriving the variables and functions shown in Table 3.3, according to the node state model which will be presented in Section 3.2.4, we have the following relationships:

$$Q_{s_s} = \pi_s, \tag{3.5}$$

$$Q_{s_i} \in \{\pi_w, \pi_s, \pi_f\}, \tag{3.6}$$

$$T_{s_i} \in \{T_w, T_s, T_f\}. \tag{3.7}$$

where π_s, π_w and π_f are the steady-state probabilities of node states, and T_w, T_s and T_f are the duration times of node states, as defined in Table 3.3.

Thus we derive C from the definition form in Equation (3.4) to be:

$$C = B_w \frac{\pi_s T_{DATA}}{\pi_w T_w + \pi_s T_s + \pi_f T_f}. \tag{3.8}$$

Since B_w and T_{DATA} are known, in order to analyze C, we need to analyze π_s, π_w, π_f, T_w, T_s, and T_f. Next, we give the steps to derive these functions.

1. We use the iteration method to calculate p_t. At first we give p_t an initial value p_t^*, then the iteration process is shown in Figure 3.1. We use an error control value ε to determine the difference between p_t and p_t^*. Last we can obtain an approximate value for p_t. Since in the input values, p and R_s are the only independent variables, we can consider p_t as a function of p and R_s.

2. With p_t calculated from the last step, we can derive π_s, π_w, π_f, T_w, T_s, and T_f. Then C can be derived. This is shown in Figure 3.2. In the input values, R_s is an

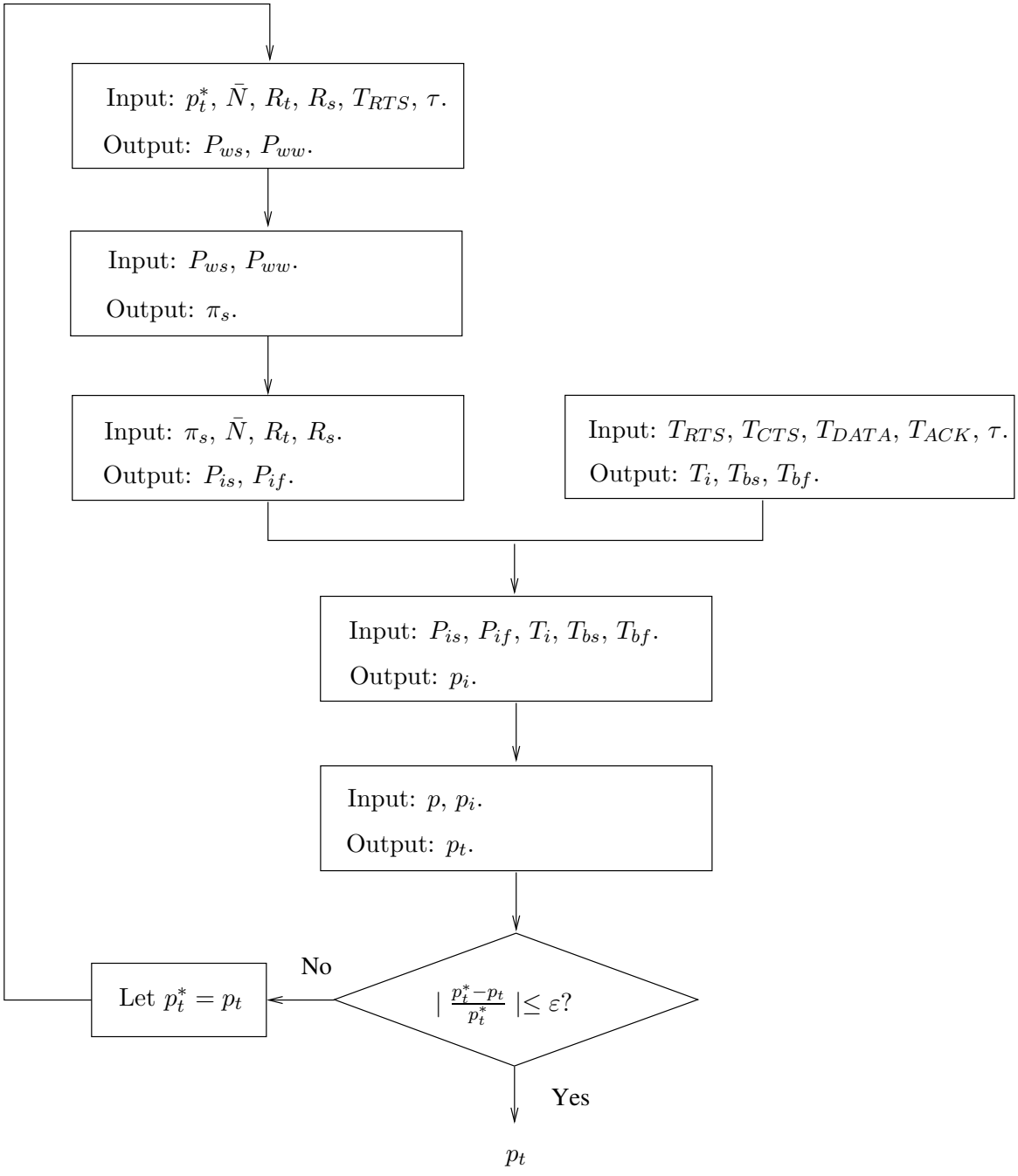

Figure 3.1: Calculation of p_t.

independent variable, p_t is a function of p and R_s, $\bar{T}_b$ is derived from p_t and R_s, and thus also a function of p and R_s. We also notice that $\bar{T}_b$ varies with different back-off mechanisms. Thus we can consider C as a function of p, R_s and $\bar{T}_b$.

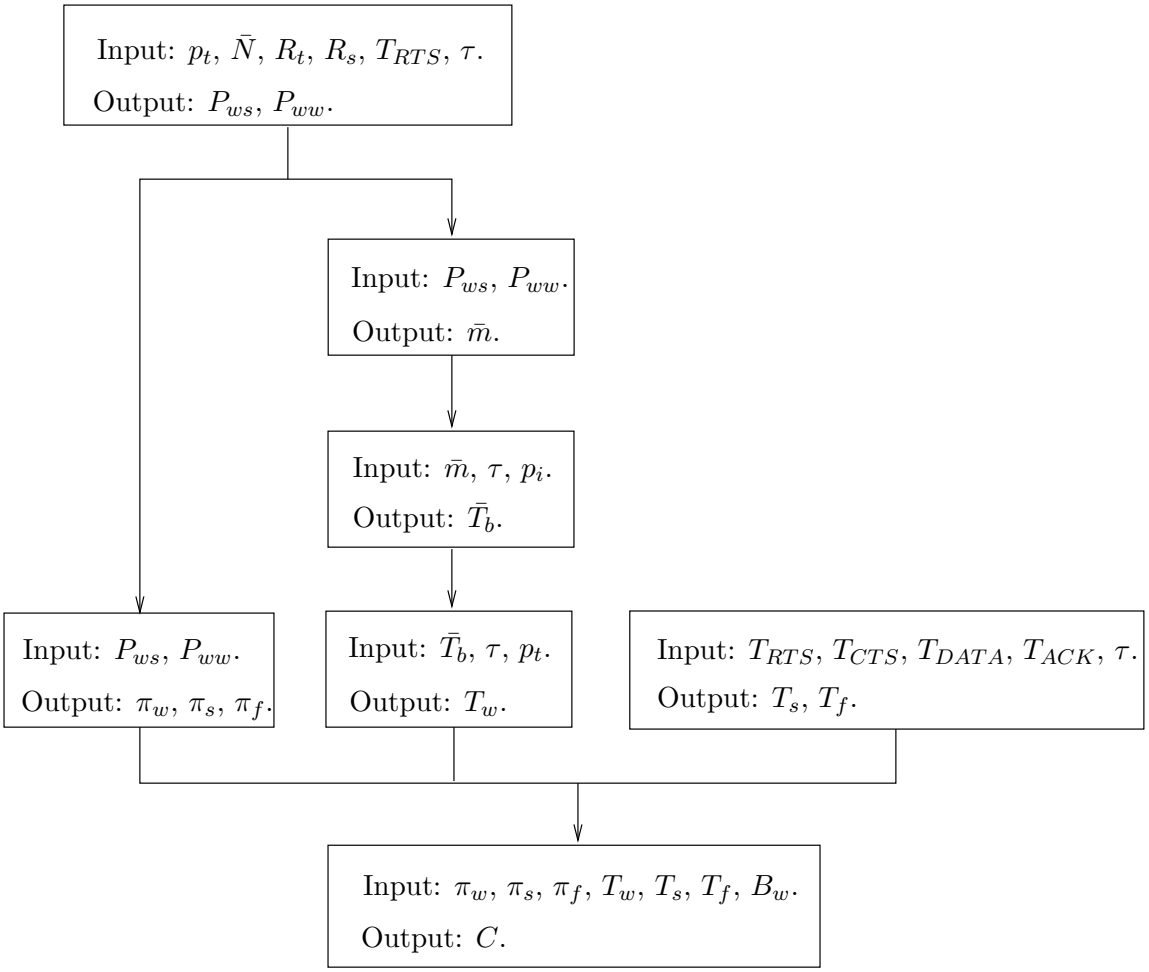

Figure 3.2: Derivation of C.

In summary, we define the capacity of MANETs C to be a function of p, R_s and $\bar{T}_b$. According to Equation (3.4), to evaluate C, we must evaluate Q_{s_i} and T_{s_i}, hence we introduce the analytical models, assumptions, and notions in the next section.

3.2 Assumptions and Models

We have given our definition of the capacity in the above section. In this section, we present the analytical models which will be used in our capacity analysis, consisting of three separate models, i.e., topology model, channel state model, and node state model. Before we present these models, we have to introduce some assumptions of the network.

3.2.1 Assumptions of the Network

Below we give the assumptions and associated parameters and variables used in our analysis. We consider a generic multi-hop network which is the same as the one used in [46] except that we choose a different MAC protocol, as described in the following.

1. We assume that the terminals in the network are distributed as a two-dimensional Poisson process with mean $\bar{N}$, i.e., the probability of finding x nodes in the sensing range of each node is given by $\bar{N}^x e^{-\bar{N}}/x!$, where $\bar{N}$ is the average number of nodes within the sensing range of each node.

2. All the nodes in the network transmit in a single channel.

3. As stated in Section 2.1, the MAC protocol used in our analysis is based on IEEE 802.11 DCF [56] and FAMA [19], and is modified for more general application. The general framework for the MAC protocol is as follows. Each node senses the channel before transmits. If the channel is found to be busy, the node defers its transmission and continues to sense the channel until it is idle. When the channel is idle, the node begins its transmission with the persistent probability p. With a probability $1 - p$ it defers until the next slot. The transmission process uses the four-way RTS/CTS/DATA/ACK handshake, which is the same as the four-way handshake in the 802.11 MAC protocol. If the transmission is unsuccessful, the node will back off a period of time $\bar{T_b}$ to retransmit. Three different back-off mechanisms are used for comparison, i.e., BEB [56], MILD [4], and EIED [45], which were described in Section 2.1.4.

4. All the nodes use the same and fixed transmission and receiving range of radius R_t, within which a packet is successfully received if there is no interference from other nodes. All the nodes use the same and fixed sensing range of radius R_s, within which a transmitter triggers carrier sense detection. Because the signal power required for carrier sense is much lower than that for transmission, R_s can be much larger than R_t.

5. For convenience, the time in our network is slotted. The length of each time slot is denoted by τ, which includes propagation delay as well as the overhead such as the transmit-to-receive turn-around time, carrier sensing delay and processing time. Hence τ represents the time required for all the nodes within the transmission range to know the event that occurred τ seconds ago. The transmission times of RTS, CTS, DATA, and ACK frames are denoted by T_{RTS}, T_{CTS}, T_{DATA}, and T_{ACK}, respectively. For the sake of simplicity, we also assume that all frame transmission times are multiples of the length of a time slot.

6. The system is independent from slot to slot during idle period, i.e., whenever there is a frame waiting to be sent, it is equally likely that this frame will be sent no matter whether it is a new frame or a retransmission frame.

7. The capacity analysis is based on a heavy-traffic assumption, i.e., each node always has a packet in its buffer to be sent except during their transmissions. and the destination node is chosen randomly from one of its neighbors. This is a fair assumption for MANETs in which nodes are relaying data continually.

8. When a node is transmitting, it cannot receive at the same time.

With the above assumptions, we present our analytical models in the following sections.

3.2.2 Topology Model

When deriving the transition probabilities in our later analysis, the formula $\bar{N}^x e^{-\bar{N}}/x!$ will be used frequently, in which $\bar{N}$ is an unknown variable. In order to calculate $\bar{N}$, node density is used in some existing analysis [33, 53, 59]. To obtain the node density, the information about the total number of nodes in the network and the whole area size is needed. However, it is not easy to obtain the information about the area size in an actual MANET, since it varies with the locations of the nodes. To address this issue, we use another parameter $\bar{k}$, the average number of neighbors of each node within its sensing range, to calculate $\bar{N}$. The definition of $\bar{k}$ refers to the notation in [55]: A simple n-vertex graph G is strongly regular if there are parameters k, λ, μ (denoted by (n, k, λ, μ)) such that G is k-regular(i.e. all the number of edges which touch each vertex are the same number k), every adjacent pair of vertices have λ common neighbors, and every nonadjacent pair of vertices have μ common neighbors.

To obtain $\bar{k}$, we model the topology of an MANET by an undirected graph $G(V, A)$. V denotes the node set in the network and A is an adjacency matrix that describes the topology of the network. An adjacency matrix is a {0,1} matrix. If G' is a relation on some n-element set $X = \{x_1, x_2, ..., x_n\}$ then G' is completely described by an $n \times n$ matrix $A = (a_{ij})$, where $a_{ij} = 1$ if x_i, x_j belong to the relation G', and otherwise $a_{ij} = 0$ [35]. In our case, X is the set of nodes, "1" denotes two corresponding nodes are in the sensing range of each other, "0" denotes they are not, and $a_{ii} = 0$. Then $\bar{k}$ is calculated by

$$\bar{k} = \frac{\sum_{i,j \in (1,n)} a_{ij}}{n}. \tag{3.9}$$

With $\bar{k}$ derived from Equation (3.9), we can easily obtain $\bar{N}$ from the relationship

$$\bar{N} = \bar{k} + 1. \tag{3.10}$$

For example, in Figure 3.3, there are six nodes in an MANET, connected by dashed lines which denote two nodes are within the sensing range of each other. The adjacency matrix A is shown in Figure 3.4. According to Equation (3.9) we have $\bar{k} \approx 1.67$. Then from Equation (3.10), $\bar{N} = 2.67$.

According to Equation (3.9), $\bar{k}$ is determined by the distribution and number of nodes, which are not related with MAC. Thus we consider $\bar{k}$ a known value, and therefore N is also known.

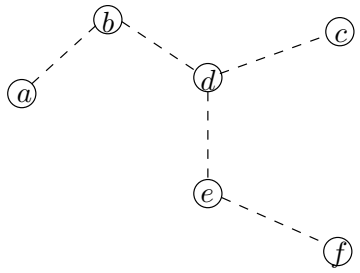

Figure 3.3: Network Topology.

$$A = \begin{array}{c|cccccc} & a & b & c & d & e & f \\ \hline a & 0 & 1 & 0 & 0 & 0 & 0 \\ b & 1 & 0 & 0 & 1 & 0 & 0 \\ c & 0 & 0 & 0 & 1 & 0 & 0 \\ d & 0 & 1 & 1 & 0 & 1 & 0 \\ e & 0 & 0 & 0 & 1 & 0 & 1 \\ f & 0 & 0 & 0 & 0 & 1 & 0 \end{array}$$

Figure 3.4: Adjacency Matrix.

3.2.3 Channel State Model

To characterize the channel state around a node, we set up a channel state model which is modified from the channel state model proposed by Wang and Garcia in [53]. In their model, they assume that the channel is a circular region, and the nodes within the region have weak interactions with nodes outside the region. Weak interaction means that the decision of inner nodes to transmit, defer and back off is almost unaffected by that of

outer nodes and vice versa. In other words, the channel's status is only decided by the successful and failed transmissions within the region. This assumption helps to simplify the model. However, it is impossible that the inner nodes of the channel region are unaffected by outer nodes. To consider this affection, we modify the states of their model, and illustrate the new model in Figure 3.5. The channel around a node i is modeled by a four-state Markov chain. The significance of the states of this Markov chain is the following:

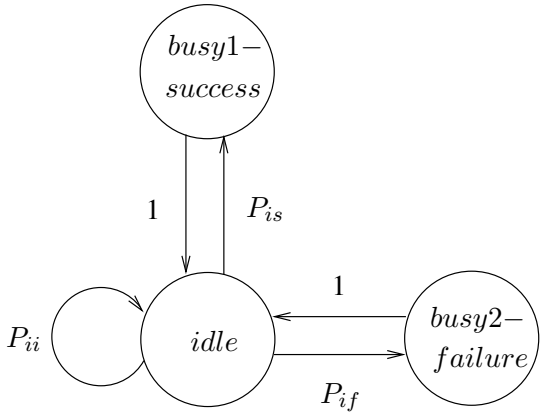

Figure 3.5: Markov Chain Model for the Channel Around Node i.

- *Idle* is the state when the channel around node i is sensed idle. Its duration is T_i.
- *Busy1-success* is the state when the channel around node i is sensed busy because at least one successful four-way handshake is in process during the same period of time. This contains two circumstances. One is that the transmitter and receiver are both within the sensing range of node i. The other one is that the transmitter (or receiver) is within the sensing range of node i, and the receiver (or transmitter) is outside the range. The duration of *busy1-success* state is T_{bs}.
- *Busy2-failure* is the state when the channel around node i is sensed busy because a node within the sensing range of node i initiates a failed handshake. For example, two

source nodes transmit RTS frames to the same destination node at the same time, and their frames collide. The duration of *busy2-failure* state is T_{bf}.

The transition probabilities between states are shown in Figure 3.5. The transition probabilities from *idle* to *idle*, from *idle* to *busy1-success*, and from *idle* to *busy2-failure* are denoted as P_{ii}, P_{is}, and P_{if}, respectively. Obviously,

$$P_{ii} + P_{is} + P_{if} = 1. \tag{3.11}$$

We will derive P_{ii}, P_{is} and P_{if} in Section 3.3.1.

Let π_i, π_{bs} and π_{bf} denote the steady-state probabilities of states *idle*, *busy1-success* and *busy2-failure*, respectively. Thus we have the following relationships:

$$\pi_i P_{is} = \pi_{bs}, \tag{3.12}$$

$$\pi_i P_{if} = \pi_{bf}. \tag{3.13}$$

3.2.4 Node State Model

In order to investigate the action of every node in different states, taking node i as an example, we adopt a three-state Markov chain to model the states of node i, shown in Figure 3.6. This model is consistent with the node state model used by Wang and Garcia in [53]. We present the three states of this Markov chain in the following:

- *Wait* is the state when node i defers for other nodes or backs off. Its duration is T_w.
- *Success* is the state when node i can complete a successful four-way handshake with other nodes. Its duration is T_s.
- *Failure* is the state when node i initiates an unsuccessful handshake with other nodes. Its duration is T_f.

By our assumption that collision avoidance is enforced at each node, no node is allowed to transmit data frames continuously, i.e., each node must transit to the *wait* state

after a successful or failed transmission. Therefore, the transition probabilities from *success* to *wait* and from *failure* to *wait* are both equal to 1. The transition probabilities from *wait* to *wait*, from *wait* to *success* and from *wait* to *failure* are denoted as P_{ww}, P_{ws}, and P_{wf}, respectively. Obviously,

$$P_{ww} + P_{ws} + P_{wf} = 1. \tag{3.14}$$

We will derive P_{ww}, P_{ws} and P_{wf} in Section 3.3.1.

Let π_w, π_s, and π_f denote the steady-state probability of state *wait*, *success*, and *failure*, respectively. Then

$$\pi_w + \pi_s + \pi_f = 1. \tag{3.15}$$

From Figure 3.6, we have

$$\begin{aligned} \pi_w P_{ww} + \pi_s + \pi_f &= \pi_w \\ \pi_w P_{ww} + 1 - \pi_w &= \pi_w \\ \pi_w &= \frac{1}{2 - P_{ww}}. \end{aligned} \tag{3.16}$$

Therefore,

$$\pi_s = \pi_w P_{ws}$$

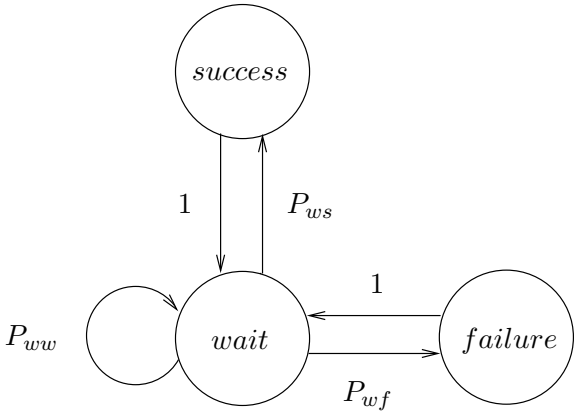

Figure 3.6: Markov Chain Model for Node i.

$$= \frac{P_{ws}}{2 - P_{ww}}, \tag{3.17}$$

$$\pi_f = 1 - \pi_w - \pi_s. \tag{3.18}$$

In summary, we have presented the assumptions and models to be used in our analysis. Next, we will analyze Q_{s_i} and T_{s_i} so that we can estimate the value of C.

3.3 Capacity Analysis of MANETs

In this section, we analyze the capacity of MANETs, in which the effects of MAC are considered in terms of the persistent probability, carrier sensing range and back-off time. The analysis is performed in two steps. The first step is to derive Q_{s_i}, i.e., π_w, π_s and π_f. The second step is to derive T_{s_i}, i.e., T_w, T_s, and T_f. Thus C can be obtained by Equation (3.8). During the analysis, we assume the following parameters are known:

1. Transmission time T_{RTS}, T_{CTS}, T_{DATA}, and T_{ACK};
2. Duration of a time slot τ;
3. Average number of nodes within R_s of node $\bar{N}$;
4. Transmission range R_t.

The following variables can be adjusted according to the MAC protocol (see Section 3.2.1) used in our analysis, so that they can be regarded as known quantities:

1. Persistent probability p, known from the carrier sense mechanism;
2. Sensing range R_s, known from the carrier sense mechanism;
3. Back-off time $\bar{T_b}$, known from the back-off mechanism BEB, MILD and EIED in Equation (3.60), (3.62) and (3.63), respectively.

3.3.1 Steady-State Probabilities of Each State of Node

To analyze the capacity C, the first step is to derive the steady-state probabilities π_s, π_w and π_f. In order to derive π_s, π_w and π_f, we will use an important function p_t. Therefore, we will obtain p_t first.

Transmission Probability of A Node

In the assumptions in Section 3.2.1, we assume that when the channel is sensed idle, in each time slot, a node intends to transmit a frame with the persistent probability p. Therefore, the probability that a node transmits in any time slot is called *transmission probability* p_t, which is defined as:

$$p_t = p \cdot p_i, \tag{3.19}$$

where p_i is the *limiting probability* (see Definition 7) that the channel is sensed in *idle* state. Note that even a node transmits, it still may fail due to collisions with other transmissions at the same time. Obviously, the capacity of the network is influenced by p_t rather than p. In our analysis, p is specified by the MAC protocol presented in Section 3.2.1. Since p_t is determined by both p and p_i, in order to obtain p_t, we need to derive p_i first.

According to the channel state model given in Section 3.2.3, the *limiting probability* p_i, i.e., the long run probability that the channel around node i is sensed idle, can be obtained by:

$$p_i = \frac{\pi_i T_i}{\pi_i T_i + \pi_{bs} T_{bs} + \pi_{bf} T_{bf}}. \tag{3.20}$$

Because $\pi_i P_{is} = \pi_{bs}$ and $\pi_i P_{if} = \pi_{bf}$, we have

$$\begin{aligned} p_i &= \frac{\pi_i T_i}{\pi_i T_i + \pi_i P_{is} T_{bs} + \pi_i P_{if} T_{bf}} \\ &= \frac{T_i}{T_i + P_{is} T_{bs} + P_{if} T_{bf}}. \end{aligned} \tag{3.21}$$

In order to calculate p_i, we need to calculate P_{is}, P_{if}, T_i, T_{bs}, and T_{bf}, respectively. We will show that P_{is} and P_{if} are functions of p_t and R_s. Thus combining Equation (3.19)

and (3.21), we will have

$$p_t^{new} = \frac{pT_i}{T_i + P_{is}(p_t, R_s)T_{bs} + P_{if}(p_t, R_s)T_{bf}}. \quad (3.22)$$

We will use the iteration method to calculate p_t. When the iteration starts, we give an initial value to p_t, denoted by p_t^*. Then we can calculate P_{is} and P_{if} using p_t^*. With P_{is}, P_{if}, T_i, T_{bs}, and T_{bf} calculated, from Equation (3.22), we obtain a new p_t, i.e., p_t^{new}. We let $p_t^* = p_t^{new}$, and recalculate P_{is} and P_{if}, then we will get another p_t^{new}. For each iteration, we compare the values of p_t and p_t^{new}. If their difference is below the error control value ε (ε is a small positive constant), we terminate the iteration and obtain an approximate value for p_t.

To perform the iteration using Equation (3.22), we first need to derive T_i, T_{bs}, and T_{bf}.

(1) Duration Time of Each Channel State: T_i, T_{bs}, and T_{bf} are the duration time of each channel state. As defined in the channel state model in Figure 3.5 in Section 3.2, *idle* is the state when the channel around node i is sensed idle. Obviously its duration is

$$T_i = \tau. \quad (3.23)$$

busy1-success is the state when at least one successful four-way handshake is done at the same time. For simplicity, we assume that the channel is in effect busy for the duration of the whole handshake, thus the busy time T_{bs} is

$$\begin{aligned} T_{bs} &= T_{RTS} + \tau + T_{CTS} + \tau + T_{DATA} + \tau + T_{ACK} + \tau \\ &= T_{RTS} + T_{CTS} + T_{DATA} + T_{ACK} + 4\tau. \end{aligned} \quad (3.24)$$

busy2-failure is the state when a node in the sensing range of node i initiates a failed handshake. Even though a CTS frame may not be sent due to the collision of the sending node's RTS frame with other frames, node i overhearing the RTS does not know if the handshake is successfully continued, until the time required for receiving a CTS frame

elapses. Therefore the channel is in effect busy, i.e., unusable for node i, for the time stated below:

$$\begin{aligned} T_{bf} &= T_{RTS} + \tau + T_{CTS} + \tau \\ &= T_{RTS} + T_{CTS} + 2\tau. \end{aligned} \tag{3.25}$$

We have derived T_i, T_{bs}, and T_{bf}. In order to calculate p_i, we still need to obtain P_{is} and P_{if}. Before that, we have to analyze π_s, since its result will be used to express P_{is} and P_{if}. From Equation (3.17), to analyze π_s, we need to analyze P_{ws} and P_{ww} first. During the analysis, p_t will show up in some functions. As we stated before, we will give an initial value to p_t, denoted by p_t^*. Thus p_t can be considered as a known value in the following analysis.

(2) Transition Probabilities P_{ws} and P_{ww}: To analyze the transition probability P_{ws} from *wait* to *success* state in Figure 3.6, we need to calculate the probability $P_{ws}(r)$ that node i successfully initiates a four-way handshake with node j at a given time slot when the distance between them is r. Before calculating $P_{ws}(r)$, we define $E(r)$ to be the region which is the part of sensing area of node j but is not covered by the sensing range of node i. $E(r)$ is called the *exclusive area*, as shown in Figure 3.7. For simplicity, in later analysis we also use the notation of a region to denote the area size of the region.

The calculation of $E(r)$ is illustrated in Figure 3.8. We define $B(r)$ to be the intersection of the sensing areas of node i and j. Then its area size

$$\begin{aligned} B(r) &= 2(\pi R_s^2 \frac{2\alpha}{2\pi} - \frac{r}{2} R_s \sin\alpha) \\ &= 2(R_s^2\alpha - \frac{2R_s\cos\alpha}{2} R_s \sin\alpha) \\ &= 2R_s^2(\alpha - \cos\alpha\sin\alpha) \\ &= 2R_s^2(\arccos(\frac{r}{2R_s}) - \cos\alpha\sqrt{1-\cos^2\alpha}) \\ &= 2R_s^2(\arccos(\frac{r}{2R_s}) - \frac{r}{2R_s}\sqrt{1-(\frac{r}{2R_s})^2}) \\ &= 2R_s^2 q(\frac{r}{2R_s}), \end{aligned} \tag{3.26}$$

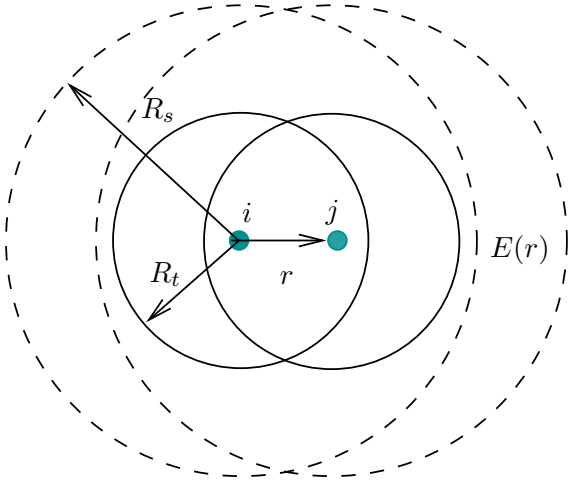

Figure 3.7: Illustration of Exclusive Area for Transmitter i and Receiver j.

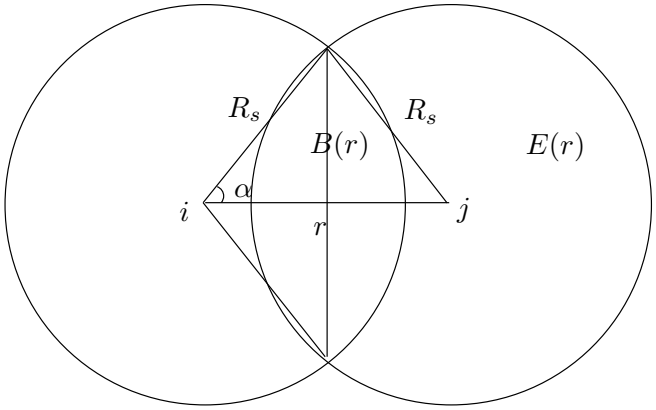

Figure 3.8: Illustration of Calculation of $E(r)$.

where $q(l) \triangleq \arccos(l) - l\sqrt{1-l^2}$. Thus

$$\begin{aligned} E(r) &= \pi R_s^2 - B(r) \\ &= \pi R_s^2 - 2R_s^2 q(\frac{r}{2R_s}). \end{aligned} \tag{3.27}$$

Then we can calculate $P_{ws}(r)$ using $E(r)$.

The calculation of $P_{ws}(r)$ has been studied by other researchers in [3, 53]. However, we will show that both of them are not accurate. For convenience, we use our notations to discuss their results. In [53], the authors claimed that

$$P_{ws}(r) = p_1 \cdot p_2 \cdot p_3 \cdot p_4(r), \tag{3.28}$$

where p_1 is the probability that node i transmits in a slot, p_2 is the probability that node j does not transmit in the same slot, p_3 is the probability that none of the nodes within R_s of i transmits in the same slot, $p_4(r)$ is the probability that none of the nodes in area $E(r)$ transmits for $(2T_{RTS} + \tau)$ time. In fact, node j is included in the nodes within radius R_s of node i, so we can use p_3 to replace $p_2 p_3$ in Equation (3.28). On the other hand, the time of $(2T_{RTS} + \tau)$ in $p_4(r)$ is not accurate. The authors in [53] explained that the reason for $(2T_{RTS} + \tau)$ is that the vulnerable period for an RTS is $(2T_{RTS} + \tau)$. However, for slotted MAC protocols, the vulnerable period for an RTS should be $(T_{RTS} + \tau)$. This is because if another node within area $E(r)$ transmits after node i begins to transmit RTS and before the end of sensing time τ following the RTS, a collision will occur, as illustrated in Figure 3.9. Once the RTS is received successfully by the destination node (which can then start sending the CTS), the probability of further collisions is assumed to be negligibly small.

The authors in [3] used another method to calculate the probability of successful transmission, which is the counterpart of P_{ws} in our analysis. They argued that $P_{ws}(r)$ should be:

$$P_{ws}(r) = p_1' \cdot p_2'(r) \cdot p_3' \cdot p_4' \cdot p_5'(r) \cdot p_6'(r), \tag{3.29}$$

where p_1' is the probability that node i transmits an RTS in a given slot, $p_2'(r)$ is the probability that no node in area $E(r)$ is involved in communication, p_3' is the probability that no RTS transmission is in the intersection of the sensing ranges of transmitter i and

receiver j in the given slot, p'_4 is the probability that no CTS transmission is in the given slot, given that there was no RTS transmission in the intersection of the sensing ranges of transmitter i and receiver j, $p'_5(r)$ is the probability that no RTS transmission is in area $E(r)$ during the vulnerable period, $p'_6(r)$ is the probability that no CTS transmission is in area $E(r)$ given that there was no RTS transmission in that area during the vulnerable period.

Comparing Equation (3.28) with (3.29), we can find that they are actually equivalent. In Equation (3.29), p'_1 is equal to p_1 in Equation (3.28). Meanwhile, in Equation (3.29), $p'_3p'_4$ is equal to the probability that there are no RTS and CTS transmissions in the intersection of the sensing ranges of transmitter i and receiver j in the given slot. We also note that in Equation (3.29) $p'_2(r)$ and $p'_3p'_4$ are independent probabilities, so $p'_2(r)p'_3p'_4$ is equal to the probability that there are no RTS and CTS transmissions in the sensing range of node j. Because the sensing range of node i is the same as that of node j, $p'_2(r)p'_3p'_4$ is also equal to the probability that there are no RTS and CTS transmissions in the sensing range of node i. Hence $p'_2(r)p'_3p'_4$ in Equation (3.29) is equal to p_3 in Equation (3.28). Last, in Equation (3.29), $p'_5(r)p'_6(r)$ is equal to the probability that there are no RTS and CTS transmissions in area $E(r)$ during the vulnerable period, which is equal to $p_4(r)$ in Equation (3.28).

Based on the above discussion, we conclude that $P_{ws}(r)$ should be given by:

$$P_{ws}(r) = P_1 \cdot P_2 \cdot P_3(r), \tag{3.30}$$

where P_1 is the probability that node i transmits in a slot, P_2 is the probability that node j and all the other nodes except node i within R_s of node i does not transmit in the same slot, $P_3(r)$ is the probability that none of the nodes in area $E(r)$ transmits for $(T_{RTS} + \tau)$ time.

From the definition of p_t^*, we have $P_1 = p_t^*$. Next we derive P_2 using the Poisson distribution of the nodes. According to the Poisson distribution, the probability of having x nodes within the sensing range R_s of node i is $\bar{N}^x e^{-\bar{N}}/x!$, where $\bar{N}$ is the average number of nodes within the sensing range of node i. We have derived $\bar{N}$ from Equation (3.10)

in Section 3.2.2. Assuming that each node transmits independently, the probability that $(x-1)$ nodes within the sensing range of node i keep silent in a time slot is $(1-p_t)^{x-1}$, where $(1-p_t)$ is the probability that a node does not transmit in a time slot. Thus P_2 is given by

$$\begin{aligned}
P_2 &= \sum_{x=2}^{\infty}(1-p_t^*)^{x-1}\frac{\bar{N}^x}{x!}e^{-\bar{N}} \\
&= \sum_{x=2}^{\infty}\frac{1}{1-p_t^*}\frac{[(1-p_t^*)\bar{N}]^x}{x!}e^{-\bar{N}} \\
&= \frac{e^{-p_t^*\bar{N}}}{1-p_t^*}\sum_{x=2}^{\infty}\frac{[(1-p_t^*)\bar{N}]^x}{x!}e^{-(1-p_t^*)\bar{N}} \\
&= \frac{e^{-p_t^*\bar{N}}}{1-p_t^*}\{\sum_{x=0}^{\infty}\frac{[(1-p_t^*)\bar{N}]^x}{x!}e^{-(1-p_t^*)\bar{N}} - e^{-(1-p_t^*)\bar{N}} - (1-p_t^*)\bar{N}e^{-(1-p_t^*)\bar{N}}\} \\
&= \frac{e^{-p_t^*\bar{N}}}{1-p_t^*}[1-e^{-(1-p_t^*)\bar{N}} - (1-p_t^*)\bar{N}e^{-(1-p_t^*)\bar{N}}] \\
&= \frac{e^{-p_t^*\bar{N}} - e^{-\bar{N}}}{1-p_t^*} - \bar{N}e^{-\bar{N}}. \qquad (3.31)
\end{aligned}$$

Similarly, the probability that none of the terminals in $E(r)$ transmits in a time slot is given by

$$\begin{aligned}
p_3(r) &= \sum_{x=0}^{\infty}(1-p_t^*)^x\frac{(\frac{E(r)}{\pi R_s^2}\times\bar{N})^x}{x!}e^{-\frac{E(r)}{\pi R_s^2}\times\bar{N}} \\
&= e^{-p_t^*\bar{N}\frac{E(r)}{\pi R_s^2}}. \qquad (3.32)
\end{aligned}$$

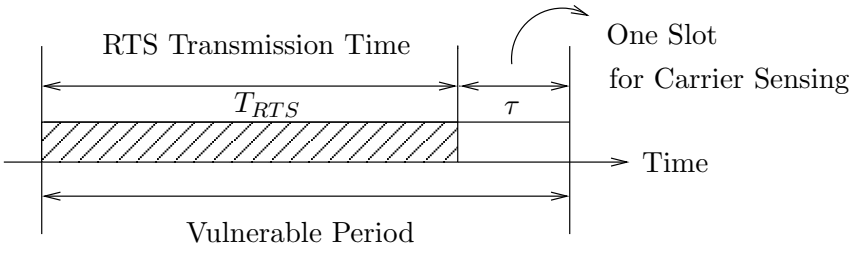

Figure 3.9: Vulnerable Period for RTS.

Thus,

$$\begin{aligned} P_3(r) &= (p_3(r))^{T_{RTS}+\tau} \\ &= e^{-p_t^* \bar{N}(T_{RTS}+\tau)\frac{E(r)}{\pi R_s^2}}. \end{aligned} \tag{3.33}$$

Given that each sending node chooses any one of its neighbors as the receiver with equal probability, r can be considered as a uniform random variable in the range $0 < r < R_t$. Then, the probability density function of the distance r between node i and j is

$$f(r) = \frac{1}{R_t}. \tag{3.34}$$

From the total probability theorem [52], we can write P_{ws} as follows:

$$\begin{aligned} P_{ws} &= \int_0^{R_t} f(r) P_{ws}(r) dr \\ &= \int_0^{R_t} \frac{1}{R_t} p_t^* \left(\frac{e^{-p_t^*\bar{N}} - e^{-\bar{N}}}{1-p_t^*} - \bar{N}e^{-\bar{N}}\right) e^{-p_t^*\bar{N}(T_{RTS}+\tau)\frac{E(r)}{\pi R_s^2}} dr \\ &= \frac{p_t^*}{R_t}\left(\frac{e^{-p_t^*\bar{N}} - e^{-\bar{N}}}{1-p_t^*} - \bar{N}e^{-\bar{N}}\right) \int_0^{R_t} e^{-p_t^*\bar{N}(T_{RTS}+\tau)\frac{E(r)}{\pi R_s^2}} dr \\ &= \frac{p_t^*}{R_t} p_t^* \left(\frac{e^{-p_t^*\bar{N}} - e^{-\bar{N}}}{1-p_t^*} - \bar{N}e^{-\bar{N}}\right) \int_0^{R_t} e^{-p_t^*\bar{N}(T_{RTS}+\tau)[1-2q(\frac{r}{2R_s})/\pi]} dr. \end{aligned} \tag{3.35}$$

In Equation (3.35), R_t, T_{RTS} and τ are known parameters, $\bar{N}$ is derived from constant k in Equation (3.10), R_s is an independent variable, and p_t^* is the value for iteration. Thus P_{ws} is the function of p_t^* and R_s, and can be written as $P_{ws}(p_t^*, R_s)$.

In order to analyze P_{ww}, we define $\bar{M}$ to be the average number of nodes within the transmission range of node i. Since when the node density does not change, the number of nodes is proportional to the area size,

$$\begin{aligned} \bar{M} &= \frac{\bar{N}\pi R_t^2}{\pi R_s^2} \\ &= \frac{\bar{N}R^2}{R_s^2}. \end{aligned} \tag{3.36}$$

From the Markov chain shown in Figure 3.6, the transition probability P_{ww} that node i continues to stay in *wait* state in a slot is the probability that node i does not initiate

any transmission and there is no node within the transmission range of node i initiating a transmission.

$$\begin{aligned} P_{ww} &= (1-p_t^*)\sum_{x=1}^{\infty}(1-p_t^*)^{x-1}\frac{\bar{M}^x}{x!}e^{-\bar{M}} \\ &= e^{-p_t^*\bar{M}}\sum_{x=1}^{\infty}\frac{[(1-p_t^*)\bar{M}]^x}{x!}e^{-(1-p_t^*)\bar{M}} \\ &= e^{-p_t^*\bar{M}}\{\sum_{x=0}^{\infty}\frac{[(1-p_t^*)\bar{M}]^x}{x!}e^{-(1-p_t^*)\bar{M}} - e^{-(1-p_t^*)\bar{M}}\} \\ &= e^{-p_t^*\bar{M}}(1-e^{-(1-p_t^*)\bar{M}}) \\ &= e^{-p_t^*\bar{M}} - e^{-\bar{M}}, \end{aligned} \tag{3.37}$$

In Equation (3.37), R_t is a constant, $\bar{N}$ is derived from constant k in Equation (3.10), R_s is an independent variable, and p_t^* is the value for iteration. Thus P_{ww} is the function of p_t^* and R_s, and can be written as $P_{ww}(p_t^*, R_s)$.

So far, we have obtained the expression of P_{ws} and P_{ww} in Equation (3.35) and (3.37), as the functions of p_t^* and R_s. Next, we will derive π_s which is a function of P_{ws} and P_{ww}.

(3) Steady-state Probability π_s: According to Equation (3.17) in Section 3.2.4, π_s is given by

$$\begin{aligned} \pi_s &= \frac{P_{ws}}{2-P_{ww}} \\ &= \frac{P_{ws}(p_t^*, R_s)}{2-P_{ww}(p_t^*, R_s)}. \end{aligned} \tag{3.38}$$

Thus π_s is also the function of p_t^* and R_s, and can be written as $\pi_s(p_t^*, R_s)$.

Next, we will express P_{is} and P_{if} using π_s, so that P_{is} and P_{if} are also the functions of p_t^* and R_s. Thus p_t^{new} can be calculated through (3.22), with known T_i, T_{bs}, T_{bc} and T_{bf}.

(4) Transition Probabilities P_{is} and P_{if}: In order to derive p_t^* in Equation (3.22), we will analyze P_{is} and P_{if}, i.e., the transition probabilities from *idle* to *busy1-success* and from *idle* to *busy2-failure*, as shown in Figure 3.5.

First, let us analyze the transition probability from *idle* to *busy1-success* P_{is}. The *idle* channel around node i changes to the *busy1-success* state in three circumstances. One is that node i is exposed to at least one source node which performs a successful transmission. Here "expose" means that two nodes can sense each other. Another circumstance is that node i is not exposed to a source node but it is exposed to at least one destination node which performs a successful reception. The third one is that node i itself transmits to a destination node successfully. Let P_{is1} be the probability that there is at least one successful transmission in node i's sensing area. Let P_{is2} be the probability that there is at least one successful reception in node i's sensing area. The probability that a node successfully transmits in a slot is π_s, and since on average $\bar{N}$ nodes including node i itself participate in generating a busy slot,

$$\begin{aligned} P_{is1} &= 1 - \sum_{x=1}^{\infty} (1-\pi_s)^x \frac{\bar{N}^x}{x!} e^{-\bar{N}} \\ &= 1 - e^{-\pi_s \bar{N}} \sum_{x=1}^{\infty} \frac{[(1-\pi_s)\bar{N}]^x}{x!} e^{-(1-\pi_s)\bar{N}} \\ &= 1 - e^{-\pi_s \bar{N}} \{ \sum_{x=0}^{\infty} \frac{[(1-\pi_s)\bar{N}]^x}{x!} e^{-(1-\pi_s)\bar{N}} - e^{-(1-\pi_s)\bar{N}} \} \\ &= 1 - e^{-\pi_s \bar{N}} + e^{-\bar{N}}. \end{aligned} \tag{3.39}$$

In order to eliminate the cases that node i is exposed to both receiver and transmitter, only those cases in which node i is in the *exclusive area* of a communication have to be considered. This kind of circumstance is illustrated in Figure 3.10. We define A to be the annulus region between two concentric circles of radii R_s and $(R_s + R_t)$. Obviously, the area size of A is

$$\begin{aligned} A &= \pi(R_s + R_t)^2 - \pi R_s^2 \\ &= \pi(R_t^2 + 2R_t R_s). \end{aligned} \tag{3.40}$$

Let $\bar{N}_A$ be the average number of nodes within the region A, then

$$\bar{N}_A = \frac{A}{\pi R_s^2} \bar{N}$$

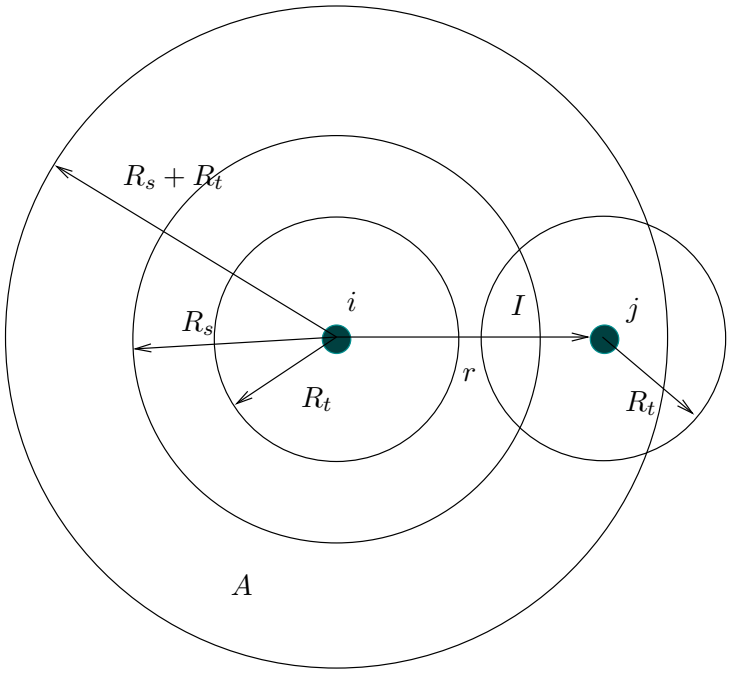

Figure 3.10: Illustration of Areas A and $I(r)$. (A is the annulus between two concentric circles of radii R_s and $(R_s + R_t)$. $I(r)$ is the intersection area of the sensing area of node i and transmission area of node j.)

$$= \frac{(R_t^2 + 2R_tR_s)\bar{N}}{R_s^2}. \tag{3.41}$$

Assume that node j in A, as shown in Figure 3.10, transmits a frame. It may choose any of its neighboring nodes as its receiver with equal probability. We define $I(r)$ to be the intersection of the sensing area of node i and transmission area of node j. Since usually R_s is not much larger than R_t, we can consider $I(r)$ as the intersection of two same circles of radius R_s. Thus in later calculation, we use the result of $B(r)$ from Equation (3.26) to approximate $I(r)$. Because π_s denotes the probability that a node begins a successful four-way handshake at each slot, the probability that j initiates a successful four-way handshake to a node in $I(r)$ is given by

$$P_I(r) = \pi_s \frac{I(r)}{\pi R_t^2}, \tag{3.42}$$

where

$$I(r) = 2R_s^2 q(\frac{r}{2R_s}). \tag{3.43}$$

The above results from the assumptions that node j chooses its destination nodes in its transmission range with equal probability and nodes in its transmission range are uniformly distributed.

Since the nodes in A are uniformly distributed and j is any randomly selected node in A, the probability density function of the distance between node i and j is

$$\begin{aligned} f(r) &= \frac{1}{(R_s + R_t) - R_s} \\ &= \frac{1}{R_t}. \end{aligned} \tag{3.44}$$

From the total probability theorem [52], the probability that any node in A initiates a successful four-way handshake to a node in $I(r)$ is given by

$$\begin{aligned} P_I &= \int_{R_s}^{R_s+R_t} P_I(r) f(r) dr \\ &= \int_{R_s}^{R_s+R_t} \pi_s \frac{I(r)}{\pi R_t^2} \frac{1}{R_t} dr \end{aligned}$$

$$= \int_{R_s}^{R_s+R_t} \pi_s \frac{2R_s^2 q(\frac{r}{2R_s})}{\pi R_t^3} dr$$
$$= \frac{2\pi_s R_s^2}{\pi R_t^3} \int_{R_s}^{R_s+R_t} q(\frac{r}{2R_s}) dr \quad (3.45)$$

The probability that at least one of the transmissions from nodes in A has a destination node in the sensing range of node i, P_{is2}, is given by

$$\begin{aligned} P_{is2} &= 1 - \sum_{x=0}^{\infty} (1-P_I)^x \frac{\bar{N}_A^x}{x!} e^{-\bar{N}_A} \\ &= 1 - e^{-P_I N_A} \sum_{x=0}^{\infty} \frac{((1-P_I)\bar{N}_A)^x}{x!} e^{-(1-P_I)\bar{N}_A} \\ &= 1 - e^{-P_I N_A}. \end{aligned} \quad (3.46)$$

Therefore, the transition probability P_{is} is given by

$$\begin{aligned} P_{is} &= P_{is1} + P_{is2} \\ &= 1 - e^{-\pi_s \bar{N}} + e^{-\bar{N}} + 1 - e^{-P_I N_A} \\ &= 2 - e^{-\pi_s \bar{N}} + e^{-\bar{N}} - e^{-P_I N_A}. \end{aligned} \quad (3.47)$$

In P_{is}, $\bar{N}$ is derived from constant k in Equation (3.10), and thus there are three variables P_I, $\bar{N}_A$ and π_s. According to Equation (3.45), there are three variables π_s, R_s and A, in P_I. From Equation (3.38), we know that π_s is the function of p_t^* and R_s. From Equation (3.40), A is the function of R_s. From Equation (3.41), $\bar{N}_A$ is the function of R_s. Therefore, P_{is} is the function of p_t^* and R_s, and can be denoted as $P_{is}(p_t^*, R_s)$.

In order to analyze the transition probability from *idle* to *busy2-failure* P_{if}, let us analyze the transition probability from *idle* to *idle* P_{ii} first, which is easier to derive. Then we can calculate P_{if} through P_{ii} and P_{is}. The *idle* channel stays in *idle* state if none of the nodes in the sensing area of node i transmits in this slot. Thus P_{ii} is given by:

$$\begin{aligned} P_{ii} &= \sum_{x=1}^{\infty} (1-p_t^*)^x \frac{\bar{N}^x}{x!} e^{-\bar{N}} \\ &= e^{-p_t^* \bar{N}} \sum_{x=0}^{\infty} \frac{[(1-p_t^*)\bar{N}]^x}{x!} e^{-(1-p_t^*)\bar{N}} - e^{-\bar{N}} \\ &= e^{-p_t^* \bar{N}} - e^{-\bar{N}}. \end{aligned} \quad (3.48)$$

In P_{ii}, $\bar{N}$ is derived from constant k in Equation (3.10), and p_t^* is the value for iteration. Thus P_{ii} is the function of p_t^* and can be denoted as $P_{ii}(p_t^*)$.

Having P_{is} and P_{ii} in Equation (3.47)-(3.48), from Equation (3.11), we can calculate P_{if} through the following relationship:

$$\begin{aligned} P_{if} &= 1 - P_{ii} - P_{is} \\ &= 1 - P_{ii}(p_t^*) - P_{is}(p_t^*, R_s). \end{aligned} \tag{3.49}$$

Thus P_{if} is also the function of p_t^* and R_s, and can be written as $P_{if}(p_t^*, R_s)$.

So far, we already obtained T_i, T_{bs}, T_{bf}, P_{is}, and P_{if} from Equation (3.23)-(3.25), (3.47) and (3.49). Therefore, we can calculate p_t^{new} from Equation (3.22):

$$p_t^{new} = \frac{pT_i}{T_i + P_{is}(p_t^*, R_s)T_{bs} + P_{if}(p_t^*, R_s)T_{bf}}. \tag{3.50}$$

Then, let $p_t^* = p_t^{new}$, and repeat the above iteration process for several times, we can at last obtain the value of p_t. From Equation (3.50), we find that p and R_s are shown up. Since p and R_s are both independent variables, we can consider p_t as a function of p and R_s, and write as $p_t(p, R_s)$.

Transition Probabilities Between States of Node

With p_t calculated from Equation (3.50), we can calculate P_{ws} and P_{ww} which are the transition probabilities between states in our Markov chain model of node in Figure 3.6.

From Equation (3.35), P_{ws} is written as:

$$P_{ws} = \frac{p_t}{R_t}\left(\frac{e^{-p_t\bar{N}} - e^{-\bar{N}}}{1 - p_t} - \bar{N}e^{-\bar{N}}\right)\int_0^{R_t} e^{-p_t\bar{N}(T_{RTS}+\tau)[1-2q(\frac{r}{2R_s})/\pi]}dr, \tag{3.51}$$

where p_t is the function of p and R_s, $\bar{N}$ is obtained from constant k in Equation (3.10), and R_t, T_{RTS} and τ are all constants. Thus P_{ws} can be derived from Equation (3.51), as a function of p and R_s, and written as $P_{ws}(p, R_s)$.

From Equation (3.37), P_{ww} is written as:

$$P_{ww} = (1 - p_t)e^{-\frac{p_t N R^2}{R_s^2}}, \tag{3.52}$$

where p_t is the function of p and R_s, $\bar{N}$ is obtained from constant k in Equation (3.10), and R_t is also a constant. Thus P_{ww} can be derived from Equation (3.52), as a function of p and R_s, and written as $P_{ww}(p, R_s)$.

Having $P_{ws}(p, R_s)$ and $P_{ww}(p, R_s)$ derived in Equation (3.51)-(3.52), next we can derive the steady-state probabilities π_w, π_s and π_f.

Steady-State Probabilities of Each State of Node

With $P_{ww}(p, R_s)$ given in Equation (3.52), we can calculate π_w from Equation (3.16):

$$\pi_w = \frac{1}{2 - P_{ww}(p, R_s)}. \tag{3.53}$$

Thus π_w is a function of p and R_s, and can be written as $\pi_w(p, R_s)$.

With $P_{ww}(p, R_s)$ given in Equation (3.52) and $P_{ws}(p, R_s)$ given in Equation (3.51), we have π_s from Equation (3.17):

$$\begin{aligned} \pi_s &= \pi_w P_{ws}(p, R_s) \\ &= \frac{P_{ws}(p, R_s)}{2 - P_{ww}(p, R_s)}. \end{aligned} \tag{3.54}$$

Thus π_s is a function of p and R_s, and can be written as $\pi_s(p, R_s)$.

Thus, with π_w and π_s derived above, we have π_f from Equation (3.18):

$$\begin{aligned} \pi_f &= 1 - \pi_w - \pi_s \\ &= \frac{1 - P_{ww}(p, R_s) - P_{ws}(p, R_s)}{2 - P_{ww}(p, R_s)}. \end{aligned} \tag{3.55}$$

Thus π_f is a function of p and R_s, and can be written as $\pi_f(p, R_s)$.

We have obtained the steady-state probabilities of each state of node, π_w, π_s and π_f. In order to derive the capacity $C(p, R_s, \bar{T}_b)$, we need to calculate the duration time of each state of node T_w, T_s and T_f shown in Equation (3.8), in the next subsection.

3.3.2 Duration Time of Each State of Node

In this subsection, we analyze the duration time of each state of node. From the definition in the node state model in Section 3.2, we know that *success* is the state when node i can complete a successful four-way handshake with other nodes, therefore its length is equal to the duration time of *busy1-success* state in the channel state model.

$$T_s = T_{bs} = T_{RTS} + T_{CTS} + T_{DATA} + T_{ACK} + 4\tau. \tag{3.56}$$

T_{RTS}, T_{CTS}, T_{DATA}, T_{ACK} and τ are determined by the physical layer [53, 59]. In our analysis, we can regard them as constants, so we can obtain T_s.

Referring to Figure 3.6, because *failure* is the state when node i initiates a failed handshake with a node within its transmission range. Therefore, its duration time is the same as T_{bf}:

$$T_f = T_{bf} = T_{RTS} + T_{CTS} + 2\tau. \tag{3.57}$$

Last, the duration time of *wait* state T_w is given by

$$T_w = \bar{T}_b + \bar{T}_d, \tag{3.58}$$

where $\bar{T}_b$ is the average back-off time, which varies with different back-off mechanisms, and $\bar{T}_d$ is the average deferring time, which is the time between the point the node senses the channel idle and the point the node transmits. In order to derive T_w, we need to derive $\bar{T}_b$ and $\bar{T}_d$ first. Because we choose three different back-off mechanisms in our MAC protocol, i.e., BEB [56], MILD [4], and EIED [45], we derive $\bar{T}_b$ for each back-off mechanism, denoted by $\bar{T}_b^{(BEB)}$, $\bar{T}_b^{(MILD)}$ and $\bar{T}_b^{(EIED)}$, respectively.

When we apply BEB in our MAC protocol, we assume $\bar{m}$ the average number of collisions for each transmission. According to the node state model in Section 3.2.4, in each time slot, the transition probability from *wait* to *success* is given by P_{ws}, and the transition probability from *wait* to *failure* is given by P_{wf}. Therefore for each successful transmission, there are average P_{wf}/P_{ws} collisions, i.e.,

$$\bar{m} = \frac{P_{wf}}{P_{ws}}$$

$$= \frac{1 - P_{ww} - P_{ws}}{P_{ws}}, \tag{3.59}$$

where P_{ws} and P_{ww} are obtained from Equation (3.51) and (3.52). With $\bar{m}$ calculated from Equation (3.59), the contention window size is $2^{\bar{m}}$. Thus, the node selects a random back-off timer uniformly distributed in $[0, 2^{\bar{m}} - 1]$. Reasonably, we choose the middle value in this period, $2^{\bar{m}-1}$, as the average back-off timer. Since the back-off timer decreases as long as the channel is sensed idle, "frozen" when a transmission is detected, and reactivated when the channel is sensed idle again, then the average back-off time for each node in one transmission is given by

$$\bar{T_b}^{(BEB)} = \frac{2^{\bar{m}-1}\tau}{p_i}, \tag{3.60}$$

where p_i is the limiting probability that the channel is sensed idle in each time slot. From Equation 3.19, we have

$$p_i = \frac{p_t}{p}, \tag{3.61}$$

where p is known, and p_t is derived from Equation (3.50), thus p_i is obtained. In Equation (3.60), τ, $\bar{m}$ and p_i are all known, thus we can derive $\bar{T_b}^{(BEB)}$.

When MILD [4] is adopted as the back-off mechanism, the back-off interval is increased by a multiplicative factor (1.5) upon a collision and decreased by 1 step upon a successful transmission, where step is defined as the transmission time of an RTS frame. We still use $\bar{m}$ to indicate the average number of collisions. Then the back-off time is

$$\bar{T_b}^{(MILD)} = \frac{(1.5\bar{m} - 1)\tau}{2p_i}, \tag{3.62}$$

where $\bar{m}$ is obtained from Equation (3.59), and τ is a constant.

As for EIED back-off mechanism [45], the contention window size is decreased by a factor r_D upon a successful transmission, and increased by a factor r_I upon a collision. The simulation results in [45] show that EIED with relatively smaller value of r_D compared to the value of r_I has higher performance gain. For example, let $r_I = 2$, and $r_D = 2^{1/8}$,

then the back-off time can be written as

$$\begin{aligned} \bar{T}_b^{(EIED)} &= \frac{\frac{1}{2} \cdot \frac{r_I}{r_D} \bar{m}\tau}{p_i} \\ &= \frac{2^{-\frac{1}{8}} \bar{m}\tau}{p_i}, \end{aligned} \tag{3.63}$$

where $\bar{m}$ is obtained from Equation (3.59), and τ is a constant.

Thus $\bar{T}_b$ is derived for three back-off mechanisms used in our MAC scheme. From Equation (3.58), in order to derive T_w, we still need to derive $\bar{T}_d$. We know that a node transmits with the transmission probability p_t in each slot, therefore the maximum number of deferring time slots for each transmission is $1/p_t$. Reasonably, we assume that the average number of deferring time slots for each transmission is a half of the maximum number, i.e., $1/(2p_t)$. p_t has been derived to be $p_t(p, R_s)$ in Equation (3.50). Then $\bar{T}_d$ is given by

$$\bar{T}_d = \frac{\tau}{2p_t(p, R_s)}. \tag{3.64}$$

Thus we can calculate T_w from

$$T_w = \bar{T}_b + \frac{\tau}{2p_t(p, R_s)}, \tag{3.65}$$

where $\bar{T}_b$ is obtained from Equation (3.60), (3.62), or (3.63), varying with different back-off mechanisms; τ is a constant; $p_t(p, R_s)$ is derived from Equation (3.50). Thus T_w is a function of p, R_s and $\bar{T}_b$, and can be written as $T_w(p, R_s, \bar{T}_b)$.

So far, we have derived the duration time of each state of node T_w, T_s, and T_f. We have also derived the steady-state probabilities π_w, π_s and π_f in Section 3.3.1. Thus we are able to derive the close form of the capacity in the next subsection.

3.3.3 Capacity Close Form

In the previous subsections, we have derived π_w, π_s, π_f, T_s, T_f and T_w needed in the capacity form (Equation (3.8)). Thus, we can derive the capacity of MANETs $C(p, R_s, \bar{T}_b)$ in the following:

$$C(p, R_s, \bar{T}_b) = B_w \frac{\pi_s(p, R_s) T_{DATA}}{\pi_w(p, R_s) T_w(p, R_s, \bar{T}_b) + \pi_s(p, R_s) T_s + \pi_f(p, R_s) T_f}. \tag{3.66}$$

In Equation (3.66), $\pi_w(p, R_s)$, $\pi_s(p, R_s)$, $\pi_f(p, R_s)$, and $T_w(p, R_s, \bar{T}_b)$ are derived in Equation (3.53)-(3.55) and (3.65). T_s and T_f are derived from Equation (3.56) and (3.57). B_w and T_{DATA} is a constant. Thus C is derived to be the function of the persistent probability p, the sensing range R_s, and the back-off time $\bar{T}_b$. For simplicity, we do not express π_w, π_s, π_f, T_w, T_s and T_f in the complete forms in Equation (3.66).

In summary, we have derived the capacity of MANETs in Equation (3.66) from the above analysis. The carrier sense mechanism (represented by p and R_s) and the back-off mechanism (represented by $\bar{T}_b$) in MAC layer are considered in the capacity form. In order to observe the effects of these MAC mechanisms on the capacity, we need to examine the relationship of the capacity and the variables p, R_s and $\bar{T}_b$. Therefore, we propose an algorithm in the next section, which will be used in our simulation in Chapter 4.

3.4 Algorithm for Simulation

We have derived the capacity close form in Equation (3.66) in Section 3.3.3, which is a function of persistent probability p, sensing range R_s, and back-off time $\bar{T}_b$. In this section, we give the algorithm which is used in our simulation to show the effects of p, R_s and T_b on the capacity. The results will tell us under what conditions the capacity achieves its maximum value. In order to observe the results one by one, each time we change one item of p, R_s and $\bar{T}_b$, and fix the other two. Below we take the algorithm for the effect of persistent probability on capacity as an example to illustrate this process. The algorithms for the effect of sensing range on capacity and the effect of back-off time on capacity are similar to it.

The algorithm for the effect of persistent probability on capacity is shown in Table 3.4. According to the derivation steps in Section 3.3, we compute the variables listed in Table 3.3, and at last compute the capacity. In order to obtain the relationship of the capacity C and persistent probability p, we fix R_s and $\bar{T}_b$ by giving a fixed value to R_s and adopting the BEB back-off mechanism. For readers' convenience, we give the notation for each step included by "/*" and "*/", which is consistent with the steps we presented in

Section 3.1.2.

There are three main iterations in the algorithm, noted by (1)-(3) in Table 3.4. Iteration (1) changes the value of $\bar{k}$. The average number of neighbors in the sensing range of each node $\bar{k}$ is a parameter in our analysis (see Table 3.2). Some literature [42, 51, 62] show that the number of neighbors will affect the capacity of network. In order to examine whether the effects of p, R_s and $\bar{T_b}$ on the capacity are affected by $\bar{k}$, we assume three reasonable values of $\bar{k}$ for each of the three MAC variables. Iteration (2) changes the value of p, which has 20 values in [0.01, 1] with step 0.05. We calculate C for each value of p, thus we can observe the effect of persistent probability on capacity. Iteration (3) iterates p_t and verifies if the difference of p_t and p_t^{new} is smaller than the error control value ε. If so, p_t is found and the iteration terminates. Through Iteration (3), we obtain p_t. Then through Iteration (2), we calculate C with varying p, thus we can observe the effect of p on the capacity. Finally, through Iteration (1), we can observe the effect of p on the capacity with different $\bar{k}$.

On the other hand, with different transmission range R_t and different size of DATA frames T_{DATA}, the effect of p on the capacity varies, too. We can examine these circumstances using the same algorithm, except that in Iteration (1) we only change the value of R_t and T_{DATA}, instead of $\bar{k}$.

For the effect of sensing range R_s on capacity, we fix p and $\bar{T_b}$ by giving a fixed value to p and adopting the BEB back-off mechanism. Then we let R_s vary in a range, and obtain the corresponding C. For the effect of back-off time $\bar{T_b}$ on capacity, we fix p and R_s by giving fixed values to them. Then we vary $\bar{T_b}$ by adopting three different back-off mechanisms, BEB, EIED and MILD, and obtain the corresponding C.

In summary, we defined and derived the capacity of MANETs in this chapter, and presented the algorithm for the effects of persistent probability, sensing range, and back-off time on capacity of MANETs, respectively. In the next chapter, we will perform the simulation and give the numerical results to show the effects of the MAC variables on the capacity of MANETs.

Begin
  Input constants T_{RTS}, T_{CTS}, T_{DATA}, T_{ACK}, τ, $\bar{k}$, R_t.
  Input a fixed value to variable R_s.
  Set the range of p: [0.01, 1] with step 0.05.
  Set the error control value err.

  /* Compute T_i, T_{bs}, and T_{bf}. */
  Compute $T_i = \tau$.
  Compute $T_{bs} = T_{RTS} + T_{CTS} + T_{DATA} + T_{ACK} + 4\tau$.
  Compute $T_{bf} = T_{RTS} + T_{CTS} + 2\tau$.

  For every arbitrary value of $\bar{k}$ .....(1)
    Compute $\bar{N} = \bar{k} + 1$.
    Compute $\bar{M} = \frac{\bar{N}R^2}{R_s^2}$.
    Compute $A = \pi(R_t^2 + 2R_tR_s)$.
    Compute $N_A = A\bar{N}/(\pi R_s^2)$.
    For all the integers i in [1, 20] .....(2)
      Input the initial value for p_t: $p_t^*(i)$

      /* Iteration to compute p_t. */
      For all the integers j in [1, 50] .....(3)
        Compute $P_{ww}(i)$ and $P_{ws}(i)$ from $p_t^*(i)$, $\bar{N}$, R_t, R_s, T_{RTS} and τ.
          /*P_{ww} and P_{ws} computed.*/
        Compute $\pi_s(i)$ from $P_{ww}(i)$ and $P_{ws}(i)$.
        Compute $P_{is}(i)$ and $P_{if}(i)$ from $\pi_s(i)$, $\bar{N}$, R_t and R_s.
        Compute $p_i(i)$ from $P_{is}(i)$, $P_{if}(i)$, T_i, T_{bs} and T_{bf}.
        Compute $p_t^{new}(i) = p(i)p_i(i)$.
        If the absolute value of $| \frac{p_t^*(i) - p_t^{new}(i)}{p_t^*(i)} | \leq err$,
          $p_t(i) = p_t^*(i)$.
          Exit the iteration of j.
        Else
          $p_t^*(i) = p_t^{new}(i)$.
        End
      End

(To be continued.)

(Continued.)

```
        /* Compute π_w, π_s, and π_f. */
        Compute π_w(i) from P_ww(i).
        Compute π_s(i) = π_w(i)P_ws(i).
        Compute π_f(i) = 1 − π_w(i) − π_s(i).

        /* Compute T_w, T_s, and T_f. */
        Compute m̄(i) from P_ws(i) and P_ww(i).      /* m̄ is the average number of collisions. */
        Compute T̄_b(i) from m̄(i), τ and p_i(i).     /* Back-off algorithm applied. */
        Compute T_w(i) from T̄_b(i), p_t(i) and τ.
        Compute T_s = T_RTS + T_CTS + T_DATA + T_ACK + 4τ.
        Compute T_f = T_RTS + T_CTS + 2τ.

        /* Compute C. */
        Compute C(i) from π_s(i), π_w(i), π_f(i), T_DATA, T_w(i), T_s, T_f and B_w.
      End
   End
End
```

Table 3.4: Algorithm for Relationship of Capacity and Persistent Probability.

Chapter 4

Numerical Results

We have derived the capacity of MANETs in the previous chapter. The persistent probability p, sensing range R_s and back-off time $\bar{T}_b$, representing the carrier sense and back-off mechanisms in the MAC scheme, are contained in the close form of the capacity in Equation (3.66). Thus we can adjust p, R_s and $\bar{T}_b$ to observe the effects of MAC on the capacity of MANETs. In this chapter, we present the numerical results and evaluate the effects of MAC mechanisms on the capacity of MANETs, in terms of p, R_s and $\bar{T}_b$.

4.1 Assumptions and Parameters

The numerical results are presented based on the assumptions introduced in Section 3.2 and 3.3.2. From what we assumed in Section 3.2, we have the following assumptions.

1. We consider an MANET in which the nodes are assumed to be two-dimensional Poisson distribution with the average number of nodes in the sensing range of each node $\bar{N}$. From the adjacency matrix of the network, we obtain the average number of neighbors in the sensing range of each node $\bar{k}$ according to Equation (3.9). Then, $\bar{N}$ can be

calculated by $\bar{N} = \bar{k} + 1$. Since we do not have an actual network, we just assign an estimated value for $\bar{k}$. Some literature [42, 51, 62] show that the number of neighbors will affect the capacity of the network. For example, the authors in [42] claims that for a stationary ad hoc network, the optimum connectivity is seven or eight neighbors per node. In [51, 62], it is suggested that the number of neighbors should be on the order of $\ln(N_0)$, where N_0 is the total number of nodes in the network. Thus, we give $\bar{k}$ three different values, 2, 3, and 5, to observe whether the effects of MAC on the capacity are affected by $\bar{k}$. The capacity for each value of $\bar{k}$ is calculated and drawn respectively.

2. The MAC protocol we use is a contention-based collision avoidance protocol, which adopts the carrier sense and RTS/CTS/DATA/ACK handshake mechanism in the transmission, and uses BEB, MILD or EIED back-off mechanisms to deal with the collisions. The persistent probability p and sensing range R_s in carrier sense are tunable. $\bar{T}_b$ is changed with different back-off mechanisms we use. To observe the effect of each variable on the capacity, when we change one variable, we assume the other two are fixed.

3. Referring to [53], we set the length of one time slot $\tau = 10\mu s$. The transmission times of RTS, CTS, DATA, and ACK frames are denoted by T_{RTS}, T_{CTS}, T_{DATA}, and T_{ACK}, and are all equal to $5\tau = 50\mu s$. As to the size of DATA frames, we consider two cases, $T_{DATA} = 100\tau = 1000\mu s$ and $T_{DATA} = 20\tau = 200\mu s$. The first case corresponds to a DATA frame that is much larger than the aggregate size of RTS, CTS and ACK frames. The second case corresponds to a DATA frame being only slightly larger than the aggregate size of RTS, CTS and ACK frames. In the latter case, which models networks in which radios have long turn-around times and data frames are short, it is doubtful whether a collision avoidance scheme should be employed at all, because it represents excessive overhead, which degrades the capacity.

4. Although R_s is a tunable design parameter, the transmission range R_t is usually predetermined by the hardware specification and radio signal design, and thus cannot be

Parameters for Models							
$\bar{k}$	R_t	τ	T_{DATA}	T_{ACK}	T_{RTS}	T_{CTS}	B_w
$2, 3, 5$	$100m, 120m, 150m$	$10\mu s$	$1000\mu s, 200\mu s$	$50\mu s$	$50\mu s$	$50\mu s$	$2Mbps$

Parameters for Variables						
T_i	T_{bs}	T_{bc}	T_{bf}	T_s	T_{f1}	T_{f2}
$10\mu s$	$1190\mu s^*, 390\mu s^{**}$	$60\mu s$	$120\mu s$	$1190\mu s^*, 390\mu s^{**}$	$60\mu s$	$120\mu s$

$*$ For $T_{DATA} = 100\tau = 1000\mu s$. $**$ For $T_{DATA} = 20\tau = 200\mu s$.

Table 4.1: Parameters for Evaluation on Capacity.

adjusted like R_s [16]. According to the previous study on the transmission range of MANETs [43], We assume R_t equal to 100 m, 120 m, and 150 m to observe the effects of MAC on the capacity under different transmission ranges.

5. Referring to the channel bandwidth used for simulations in [33, 53, 61], we set $B_w = 2$ Mbps, which is a reasonable value for the channel bandwidth in MANETs.

In Section 3.3.2, we derived the duration time of the states of channel and states of node. Therefore, with the parameters given above, we can calculate the parameters for duration time following the analysis in Section 3.3.2, shown in Table 4.1.

4.2 Effects of MAC protocols on Capacity of MANETs

In this section, the effects of MAC on the capacity of MANETs are evaluated in terms of the persistent probability p, sensing range R_s, and back-off time $\bar{T}_b$. For comparison, we fix the other two variables when we evaluate one variable's effect on the capacity.

4.2.1 Effect of Persistent Probability

Assuming a BEB back-off and $R_s = 150$ m, the effect of persistent probability on the capacity of MANETs is shown in Figures 4.1, 4.2, and 4.3. In these figures, we illustrate the effect of the persistent probability p on the capacity of MANETs, with different average number of neighbors $\bar{k}$, transmission range R_t, and transmission time of DATA frame T_{DATA}.

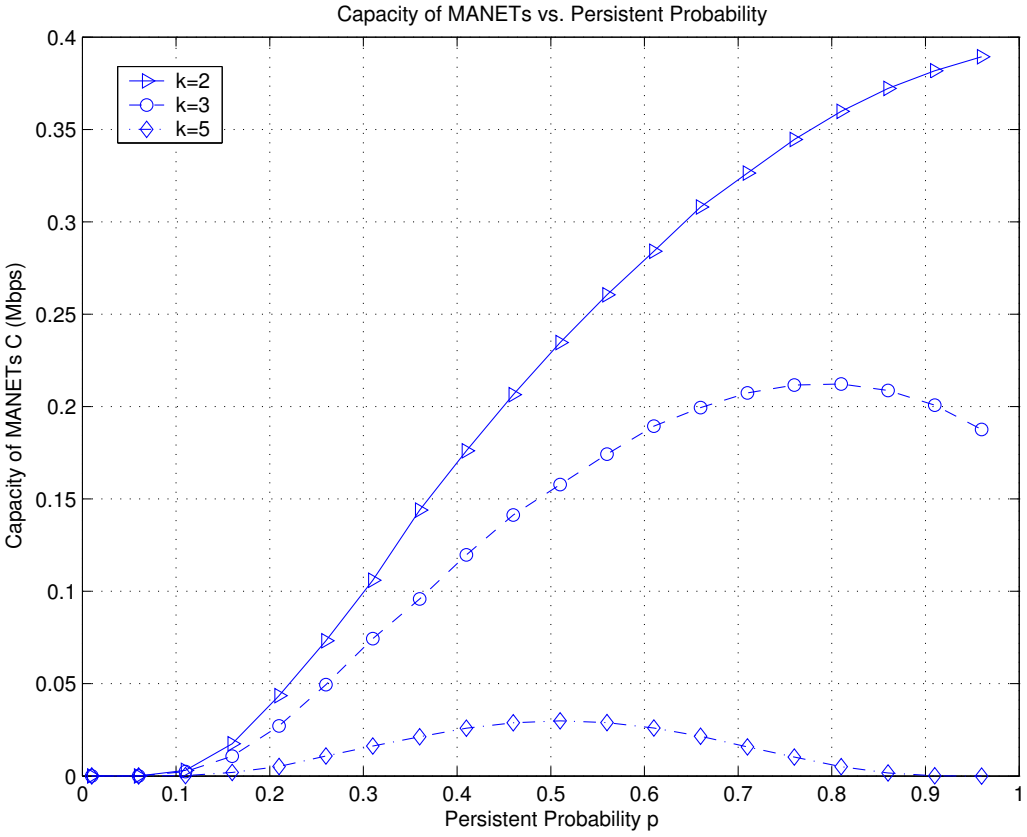

Figure 4.1: Capacity of MANETs vs. Persistent Probability with Various $\bar{k}$.

Figure 4.1 reveals the effect of persistent probability p on the capacity of MANETs, with fixed $R_t = 150$ m, $T_{DATA} = 100\tau$ and various values of $\bar{k}$. The results show that for

$\bar{k} = 2$, 3, and 5, the capacity can always achieve a maximum value at some point of p. We notice that the maximum capacity decreases when $\bar{k}$ increases because the more number of neighbors, the more collisions may happen, and the more time is needed for a successful transmission. For example, if we increase $\bar{k}$ from 3 to 5, the maximum capacity can reduce up to 85.7%. The similar result was reported in [53, 59]. Moreover, the point of p for the maximum capacity is various along with $\bar{k}$. For example, when $\bar{k} = 3$, the capacity achieves the maximum value at $p = 0.8$, while when $\bar{k} = 5$, the capacity achieves the maximum value at $p = 0.54$. This is because when the number of neighbors increases, the collisions may grow up, but a smaller persistent probability can alleviate such a trend. Thus we can achieve the maximum capacity at a smaller persistent probability.

In Figure 4.2, the effect of persistent probability p on the capacity of MANETs is shown, with fixed $\bar{k} = 3$, $T_{DATA} = 100\tau$ and various values of R_t. Similarly to Figure 4.1, the capacity also achieves a maximum value at some point of p, for $R_t = 100$ m, 120 m, and 150 m. Meanwhile, the maximum capacity increases when R_t increases because when p is high, with a larger transmission range, a node can transmit to more other nodes so as to increase the spatial reuse of the channel, which leads to a higher capacity. For example, when $R_t = 120$ m, the capacity can reach 0.08 Mbps; when $R_t = 150$ m, the capacity rises up to about 0.22 Mbps, 175% higher than the former. At the same time, we notice that no matter what R_t is, the capacity always achieves the maximum value around $p = 0.8$.

The effect of persistent probability p on the capacity of MANETs for different length of DATA frames is illustrated in Figure 4.3. In the figure, two kinds of DATA frames are assumed: $T_{DATA} = 100\tau$ and $T_{DATA} = 20\tau$. The former is the case that the data frame size is much larger than the aggregate size of RTS, CTS, and ACK frames. The latter is the case that the data frame size is only slightly larger than the aggregate size of RTS, CTS, and ACK frames. Other parameters are all the same. Obviously, when p is high, the capacity for $T_{DATA} = 20\tau$ is much lower than that for $T_{DATA} = 100\tau$. However, when p is low, the capacity for $T_{DATA} = 20\tau$ performs better than that for $T_{DATA} = 100\tau$. Thus we can conclude that when the DATA frames are short, we have to set a lower persistent probability in our MAC protocol so as to increase the capacity. Otherwise, it is not worthy

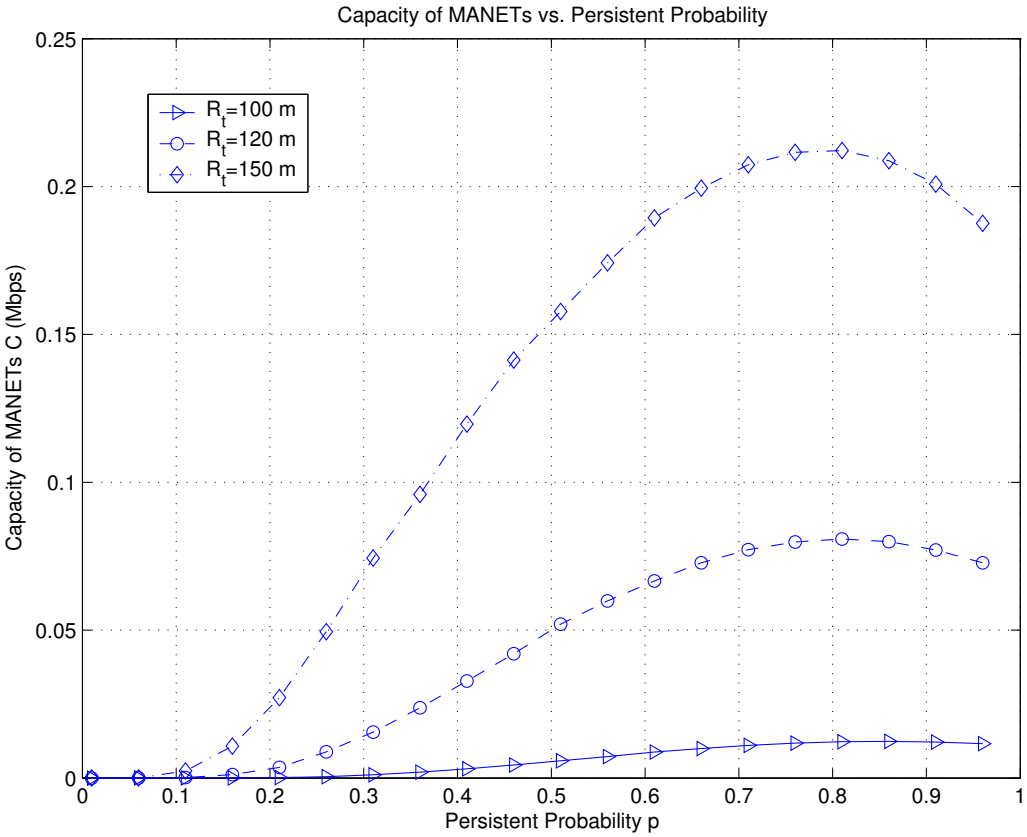

Figure 4.2: Capacity of MANETs vs. Persistent Probability with Various R_t.

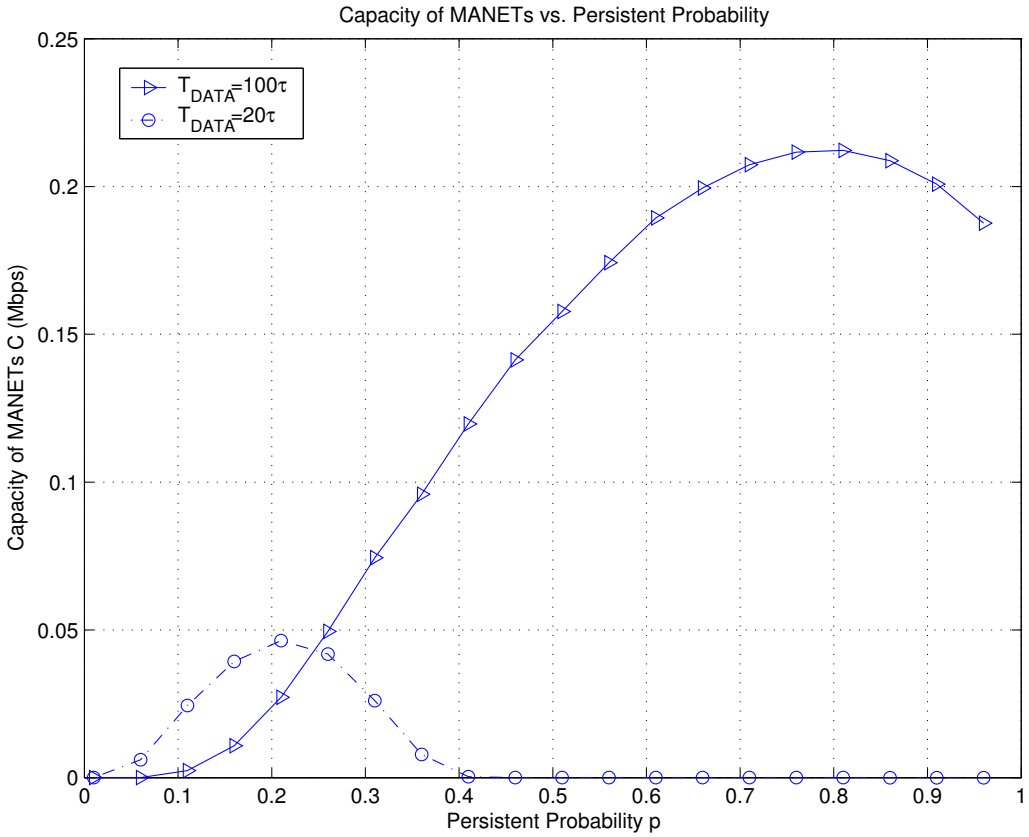

Figure 4.3: Capacity of MANETs vs. Persistent Probability with Various T_{DATA}.

to employ a collision avoidance scheme due to the proportionally larger overhead.

4.2.2 Effect of Sensing Range

The effect of sensing range on the capacity of MANETs is demonstrated in Figures 4.4, 4.5, and 4.6, assuming a BEB back-off and persistent probability $p = 0.8$. In these figures, we illustrate the relationship between the sensing range R_s and the capacity of MANETs, with different average number of neighbors $\bar{k}$, transmission range R_t, and transmission time of DATA frame T_{DATA}.

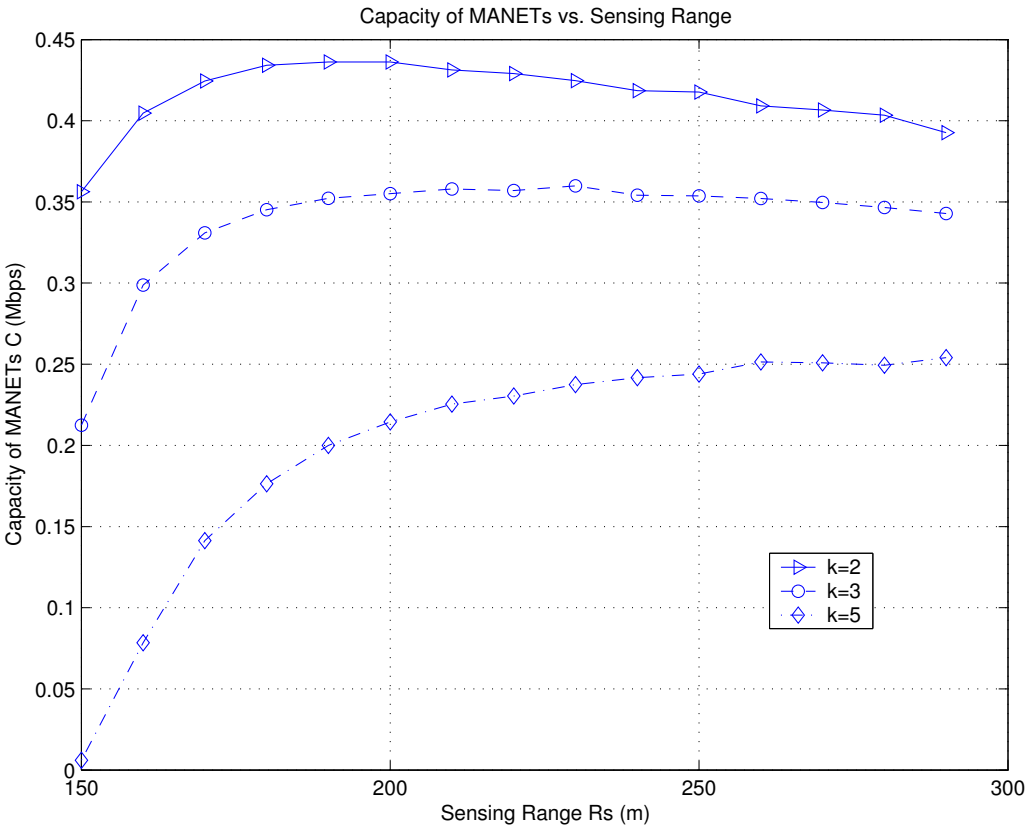

Figure 4.4: Capacity of MANETs vs. Sensing Range with Various $\bar{k}$.

Figure 4.4 shows the effect of sensing range on the capacity with different numbers of neighbors in the sensing range $\bar{k}$. We assume that the transmission range $R_t = 150$ m, and the transmission time of a DATA frame $T_{DATA} = 100\tau$. We note that for each value of $\bar{k}$, the capacity increases along with the increase of R_s when R_s is small. After a point of R_s, the capacity achieves around the maximum value, and does not make obvious changes with the increase of R_s any more. The maximum capacity decreases with the increase of the number of neighbors, because the more number of neighbors, the more collisions may happen, and the more time is needed for a successful transmission. For instance, if we increase $\bar{k}$ from 3 to 5, the maximum capacity can drop up to 22%. The similar result was reported in [16]. Moreover, the value of R_s for achieving the maximum capacity is various along with $\bar{k}$. For example, when $\bar{k} = 2$, the capacity achieves the maximum value at about $R_s = 200$ m, while when $\bar{k} = 3$, the capacity achieves the maximum value at about $R_s = 240$ m. This illustrates that the number of neighbors has to increase along with the gain of the sensing range to obtain the maximum capacity.

The effect of sensing range on the capacity of MANETs with various transmission ranges is shown in Figure 4.5. We assume that there are 3 neighbors for each node, and $T_{DATA} = 100\tau$. We have the similar observations as in Figure 4.4, i.e., the capacity increases along with the increase of R_s. In Figure 4.5, we also find that for the same R_s, the larger transmission range has a higher capacity. For example, when $R_s = 200$ m, the capacity curve for $R_t = 100$ m is 70.8% lower than the capacity curve for $R_t = 120$ m. Moreover, the capacity curve for $R_t = 150$ m rises fastest along with the increase of R_s, while the capacity curve for $R_t = 100$ m rises lowest. This indicates that the effect of sensing range on the capacity is weaken when the transmission range is short.

In Figure 4.6, we compare the different effect of sensing range on the capacity of MANETs for the two kinds of DATA frames: $T_{DATA} = 100\tau$ and $T_{DATA} = 20\tau$, while $\bar{k} = 3$ and $R_t = 150$ m. We can find that the sensing range has more obvious effect on the capacity for the case that the data frame size is much larger than the aggregate size of RTS, CTS, and ACK frames. When $T_{DATA} = 100\tau$, the capacity curve rises fast and the maximum value stays around 0.36 Mbps. When $T_{DATA} = 20\tau$, the capacity curve rises

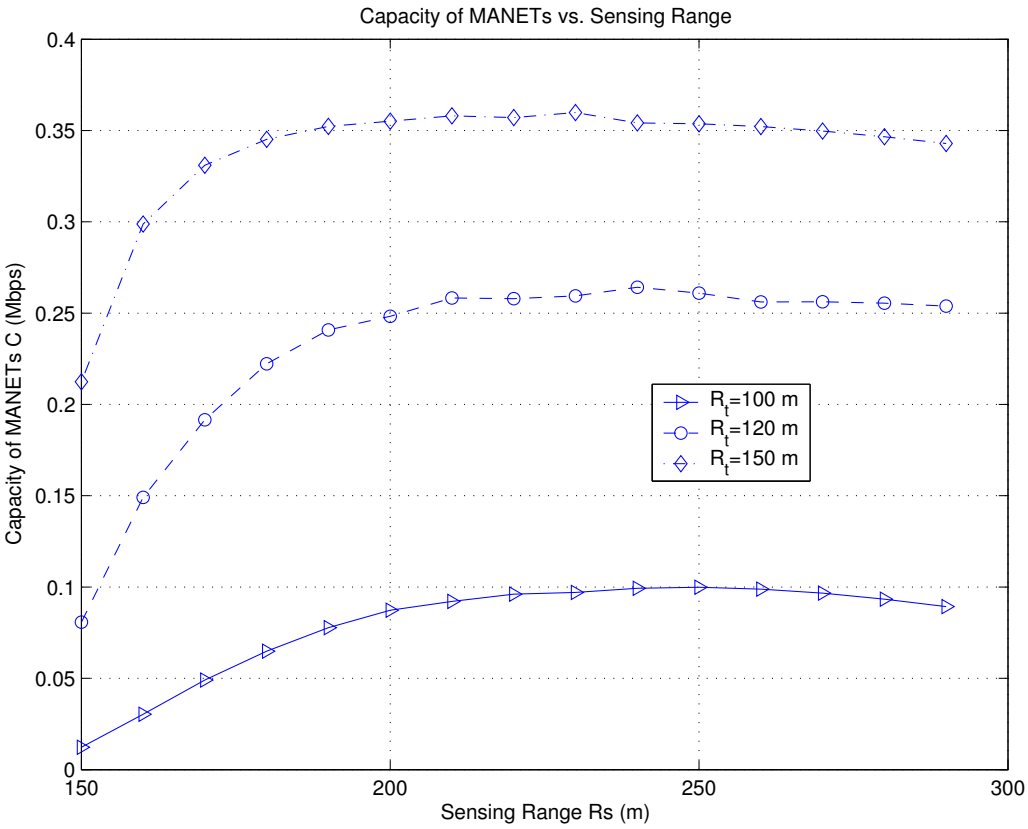

Figure 4.5: Capacity of MANETs vs. Sensing Range with Various R_t.

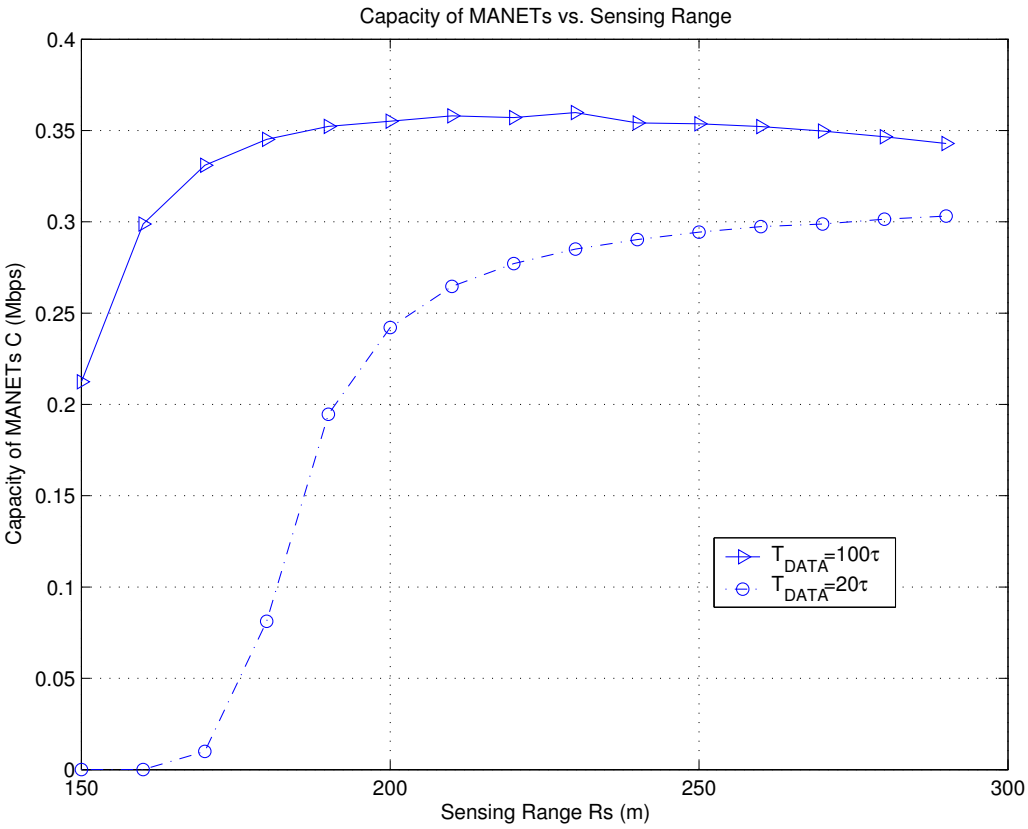

Figure 4.6: Capacity of MANETs vs. Sensing Range with Various T_{DATA}.

slowly and the maximum value is lower than that for $T_{DATA} = 100\tau$. Therefore, when the DATA frames are short, it is not worthy to employ a collision avoidance scheme due to the proportionally larger overhead.

4.2.3 Effect of Back-off Time

The effect of back-off time on the capacity of MANETs is shown in Figures 4.7, 4.8, and 4.9, in which the persistent probability $p = 0.8$, and sensing range $R_s = 150$ m. Three back-off mechanisms, BEB, MILD, and EIED, are separately adopted, and their performances are compared. In these figures, we illustrate the relationship between the back-off time $\bar{T}_b$ and the capacity of MANETs, with different average number of neighbors $\bar{k}$, transmission range R_t, and transmission time of DATA frame T_{DATA}.

Figure 4.7 reveals the effect of back-off time on the capacity for various numbers of neighbors in the sensing range of each node, assuming $R_t = 150$ m and $T_{DATA} = 100\tau$. We note that the capacity decreases with the increase of the back-off time, almost linearly. For $\bar{k} = 2$, 3, and 5, the capacity of BEB is always the lowest among the three back-off mechanisms, because the back-off time for BEB is the longest among them. The capacity of MILD is the highest, and the capacity of EIED is between that of BEB and MILD. For example, when $\bar{k} = 3$, the capacity of MILD achieves around 0.42 Mbps, while the capacity of BEB is about 0.4 Mbps, which is 4.76% lower than MILD. The capacity for the three mechanisms all drop down along with the increase of $\bar{k}$, especially for MILD. For example, the capacity of MILD is about 0.42 Mbps for $\bar{k} = 3$, but it drops down to 0.31 Mbps for $\bar{k} = 5$, reducing up to 26.2%. This is because the more number of neighbors, the more collisions in the transmissions. At the same time, the back-off time for the three mechanisms increases along with the increase of $\bar{k}$. For instance, the back-off time of BEB is $40\mu s$ when $\bar{k} = 3$, but it grows up to $59\mu s$ when $\bar{k} = 5$. This can be seen as the reason for the decrease of the capacity.

The effect of back-off time on the capacity for various transmission ranges R_t is shown in Figure 4.8, when $\bar{k} = 3$ and $T_{DATA} = 100\tau$. We note that the capacity increases

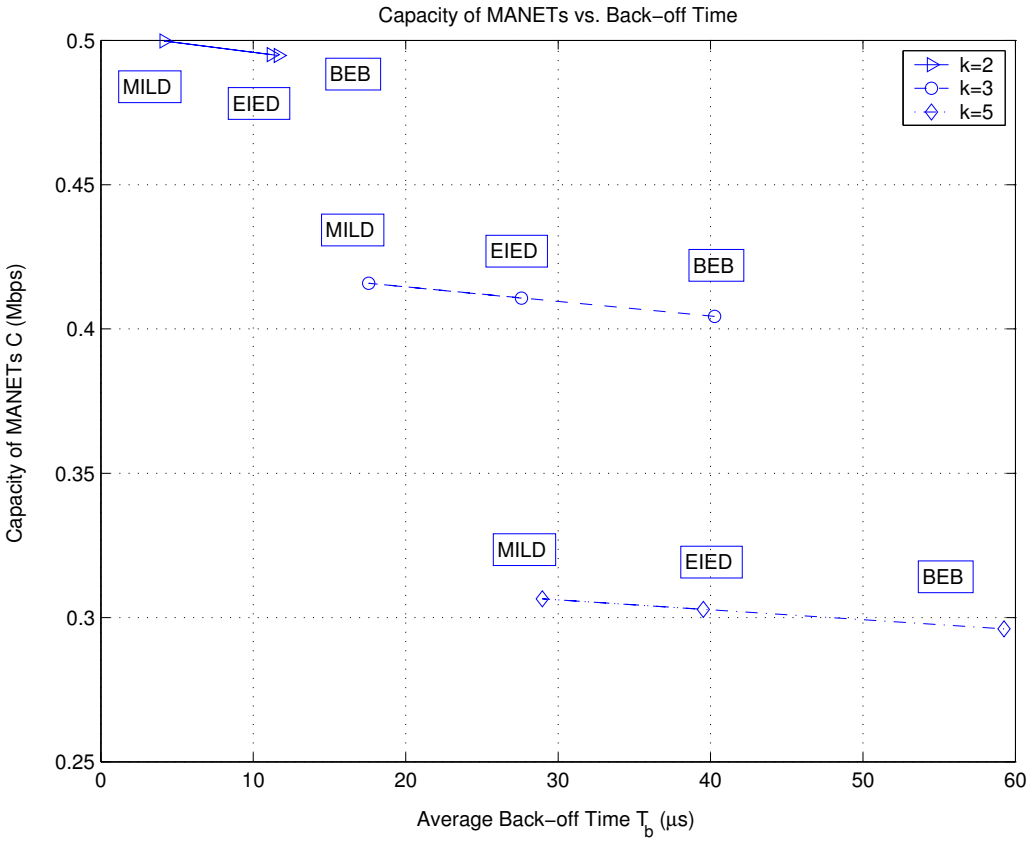

Figure 4.7: Capacity of MANETs vs. Back-off Time with Various $\bar{k}$.

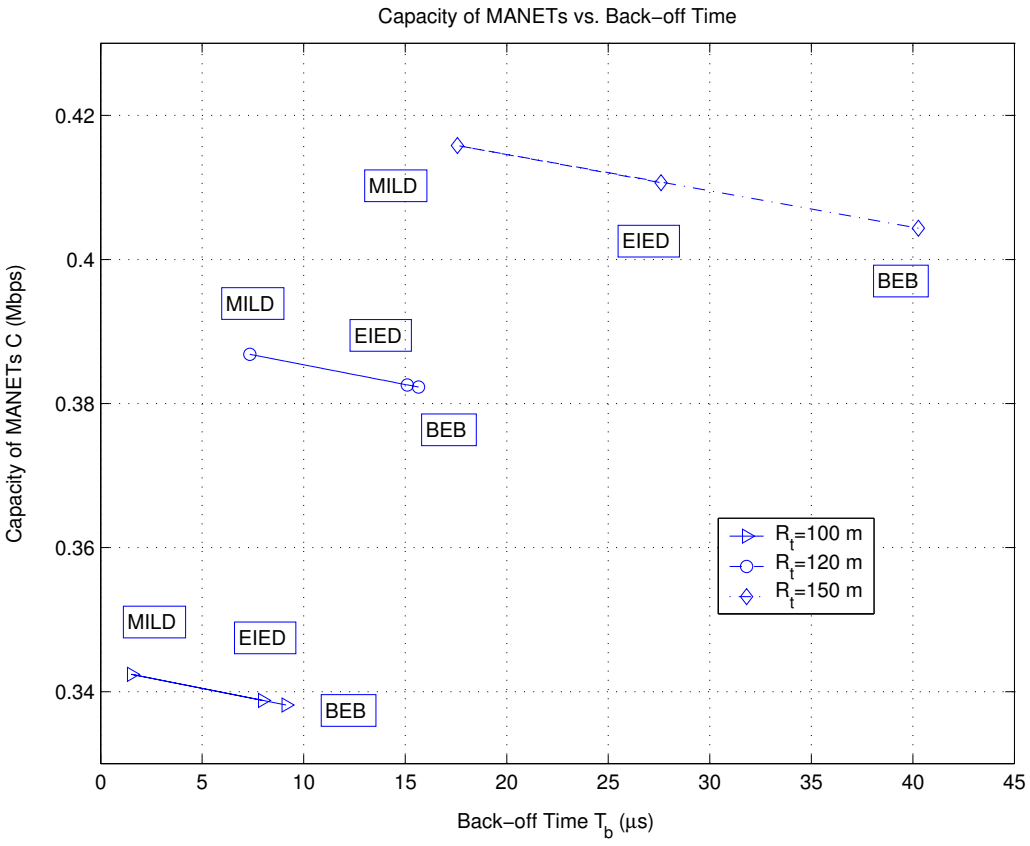

Figure 4.8: Capacity of MANETs vs. Back-off Time with Various R_t.

along with the increase of the transmission range. For instance, when $R_t = 100$ m, the capacity of MILD is about 0.342 Mbps; when $R_t = 150$ m, the capacity of MILD is about 0.415 Mbps, which is about 21.3% higher than the former. Therefore, with the same number of neighbors and sensing range, increasing the transmission rage can improve the capacity.

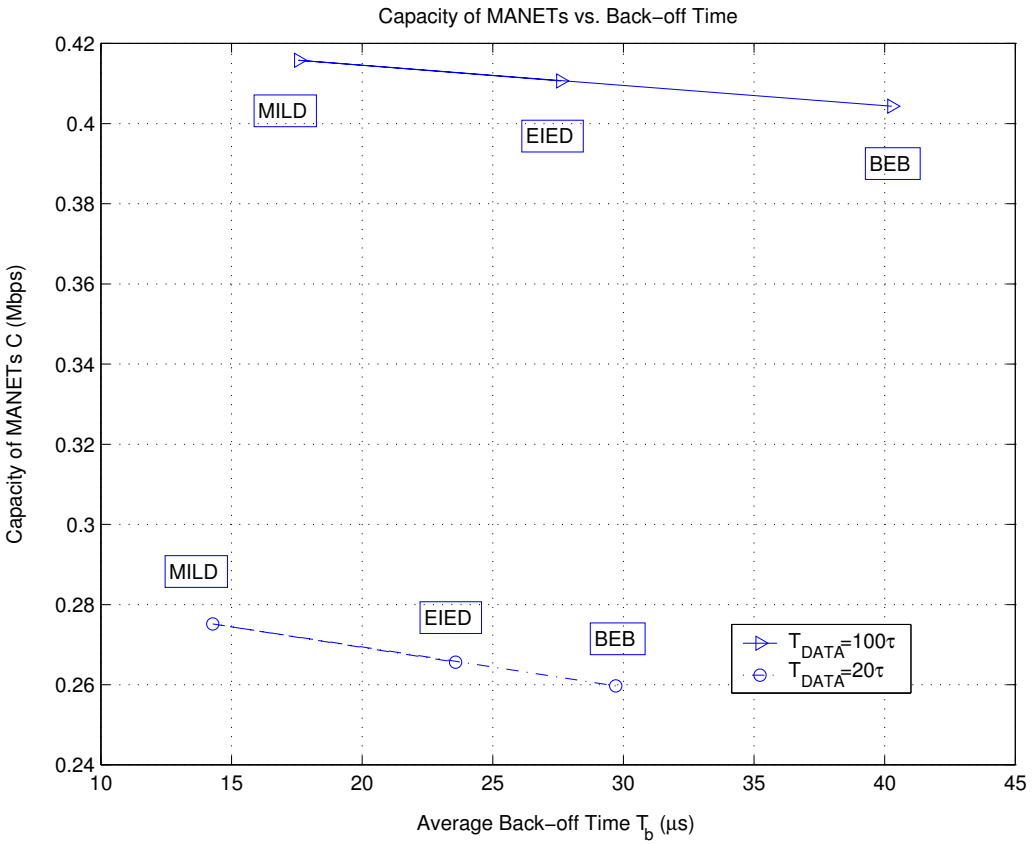

Figure 4.9: Capacity of MANETs vs. Back-off Time with Various T_{DATA}.

In Figure 4.9, the effect of back-off time on the capacity for the two kinds of DATA frames is compared: $T_{DATA} = 100\tau$ and $T_{DATA} = 20\tau$. Let $\bar{k} = 3$ and $R_t = 150$ m, we note that all the three back-off mechanisms achieve the similar capacity. When $T_{DATA} = 100\tau$, the capacity of MILD is 0.415 Mbps; when $T_{DATA} = 20\tau$, the capacity of MILD is 0.275

Mbps, which is about 33.7% lower than the former. Clearly, the capacity for the larger DATA frames is much higher than that for the shorter DATA frames. As for the back-off time, for both DATA frames, MILD requires the least time, and BEB requires the longest time. For instance, when $T_{DATA} = 100\tau$, the back-off time of BEB is $40\mu s$, and the back-off time of MILD is $17\mu s$, which is 57.5% shorter than BEB, resulting in a 5% increase of the capacity.

Chapter 5

Conclusions and Future Work

In this chapter, we present our conclusions from this thesis work and propose the future work.

5.1 Conclusions

The effects of MAC protocols on the capacity of MANETs are conducted in this thesis. MANETs have particular features and complexity compared to conventional wireless networks. This particularity requires completely different approaches to analyze the effects of MAC protocols on the capacity of MANETs.

As a prerequisite for our evaluation, we discussed the basic mechanisms of contention-based MAC protocols in MANETs. We first focused on the carrier sense, back-off, and handshake mechanisms in the IEEE 802.11 DCF protocol. Then we discussed and measured the three mechanisms separately. We proposed the sensing range and persistent probability to measure the effect of carrier sense mechanism. We used the back-off time to evaluate the effect of different back-off mechanisms. We also examined several proposed handshake mechanisms. The three mechanisms realize the goal of MAC in two aspects:

collision avoidance and spatial reuse. Since the hidden terminal problem is a main cause for collisions and the exposed terminal problem limits the spatial reuse, we discussed some solutions to the two problems. In order to analyze the MAC mechanisms in an analytical model, we examined the existing performance analysis of MAC protocols, i.e., IEEE 802.11 DCF protocol and other collision avoidance protocols. To analyze the capacity of MANETs, we selectively discussed the previous definitions and analysis of capacity. We found that significant progress has been made to evaluate the capacity of MANETs, however, it is far less sufficient for the analysis of effects of MAC on the capacity of MANETs.

After the discussion of MAC and capacity analysis, we proposed our definition of capacity of MANETs, i.e., the fraction of time in which the node is engaged in the successful transmission of data frames. Three variables of MAC, i.e., persistent probability, sensing range, and back-off time, are included in the capacity definition. To estimate the capacity of MANETs, we presented our MAC scheme and analytical models. The MAC scheme used for our analysis is a contention-based protocol, in which RTS/CTS/DATA/ACK handshake and three kinds of back-off mechanisms are adopted. Our analytical models consist of the topology model, channel state model, and node state model. The topology model considered the number of neighbors of each node, in stead of node density, making our analysis more practical. We used the Markov chain to model the channel states and node states. In the channel model, we used four states to model the sensed idle, success, and failure states of the shared channel. In the node model, we also used four states to model the wait, success, and failure states of a node. Using these models, we derived the duration time and steady-state probabilities of the states of node. Dividing the duration time of successful data transmissions by the total duration time for all the states, we estimated the capacity of MANETs according to our definition.

Since the persistent probability, sensing range, and back-off time, are included in the capacity estimation, we can adjust these MAC variables to observe their effects on the capacity. We further presented that the capacity can be maximized by tuning these variables.

Finally, numerical results were presented to evaluate the effects of those MAC

variables on the capacity of MANETs. By varying one variable while fixing the others, we evaluated the effect of persistent probability, sensing range, and back-off time on the capacity of MANETs, respectively. The results indicate that the capacity has a peak value at some point of the persistent probability, which varies with the number of neighbors, transmission range and length of data frame. At the same time, the capacity achieves the peak value for a certain sensing range, which is also influenced by the number of neighbors, transmission range and length of data frame. On the other hand, the capacity decreases along with the increase of the back-off time. Comparing the three back-off mechanisms, BEB, MILD and EIED, we noticed that MILD has the shortest back-off time and highest capacity, while BEB has the longest back-off time and lowest capacity.

5.2 Future Work

In our analysis, we assumed that all the nodes in the network use only one channel. In such a scheme, all kinds of frames, such as RTS/CTS/DATA/ACK in the IEEE 802.11 protocols, are transmitted in the same channel. There thus exist collisions between any two kinds of these frames. One common approach to reduce such collisions is to exploit the advantage of multiple channels, and transmit different kinds of frames over different separate channels [13, 15, 34, 44, 49, 60, 63, 66]. Then, a critical question that arises is: what is the optimum number of channels for each node. Therefore, an analytical model that accurately captures the effect of multi-channel MAC protocol to the capacity of MANETs is expected.

The MAC scheme we use for our analysis adopts the RTS/CTS/DATA/ACK handshake mechanism, which is sender-initiated and the main handshake mechanism used in many MAC protocols. However, there are receiver-initiated handshake mechanisms proposed for some specialized networks as shown in Section 2.1.5. Thus further analysis could be performed to address the capacity of MANETs operated in a receiver-initiated or hybrid handshake mechanism.

Although we estimate the capacity of MANETs in the framework of MAC layer,

there are many other factors influencing the capacity of MANETs, in physical layer, network layer, and transport layer. The effects of some of those factors on the capacity of MANETs have been studied, such as number of nodes, transmission power, and topology, as we presented in Section 2.4. How to establish the relationship among all of these factors in a cross-layer view can be another interesting research topic in the future.

Bibliography

[1] Research and development of mobile ad hoc networks. http://www.chinatelecom.com.cn/press.

[2] I. F. Akyildiz, X. Wang, and W. Wang. Wireless mesh networks: A survey. *Computer Networks Journal (Elsevier)*, March 2005.

[3] F. Alizadeh-Shabdiz and S. Subramaniam. MAC layer performance analysis of multi-hop ad hoc networks. In *IEEE Global Telecommunications Conference*, volume 5, pages 2781–2785, November 2004.

[4] V. Bharghavan, A. Demers, S. Shenker, and L. Zhang. MACAW: A media access protocol for wireless LAN's. In *Proc. of ACM SIGCOMM*, pages 212–225, 1994.

[5] G. Bianchi. Performance analysis of the IEEE 802.11 distributed coordination function. *IEEE Journal on Selected Areas in Communications*, 18(3):535–547, March 2000.

[6] G. Bianchi, L. Fratta, and M. Oliver. Performance evaluation and enhancement of the CSMA/CA MAC protocol for 802.11 wireless LANs. In *Proc. of IEEE International Symposium on Personal, Indoor and Mobile Radio Communications Conference*, October 1996.

[7] G. Bianchi, L. Fratta, and M. Oliveri. Performance analysis of IEEE 802.11 CSMA/CA medium access control protocol. In *Proc. of IEEE International Symposium on Personal, Indoor and Mobile Radio Communications Conference*, pages 407–411, 1996.

[8] L. Bononi, L. Budriesi, et al. A differentiated distributed coordination function MAC protocol for cluster-based wireless ad hoc networks. In *1st ACM International Workshop on Performance Evaluation of Wireless Ad Hoc, Sensor, and Ubiquitous Networks*, pages 77–86, 2004.

[9] F. Cali, M. Conti, and E. Gregori. IEEE 802.11 wireless LAN: Capacity analysis and protocol enhancement. In *Proc. of IEEE INFOCOM*, March 1998.

[10] F. Cali, M. Conti, and E. Gregori. Dynamic tuning of the IEEE 802.11 protocol to achieve a theoretical throughput limit. *IEEE/ACM Transactions on Networking*, 8(6):785–799, December 2000.

[11] F. Cali, M. Conti, and E. Gregori. IEEE 802.11 protocol: Design and performance evaluation of an adaptive backoff mechanism. *IEEE Journal on Selected Areas in Communications*, 18(9):1774–1786, September 2000.

[12] H. S. Chhaya and S. Gupta. Performance modeling of asynchronous data transfer methods of IEEE 802.11 MAC protocol. *Wireless Networks*, 3:217–234, 1997.

[13] N. Choi, Y. Seok, and Y. Choi. Multi-channel MAC protocol for mobile ad hoc networks. In *Proc. of IEEE Vehicular Technology Conference*, October 2003.

[14] B. P. Crow. Performance evaluation of the IEEE 802.11 wireless local area network protocol. Master's thesis, Department of Electrical and Computer Engineering, University of Arizona, Tucson, AZ, 1996.

[15] J. Deng and Z. J. Haas. Dual busy tone multiple access (DBTMA): A new medium access control for packet radio networks. In *Proc. of IEEE International Conference on Universal Personal Communications*, October 1998.

[16] J. Deng, B. Liang, and P. K. Varshney. Tuning the carrier sensing range of IEEE 802.11 MAC. In *IEEE Global Telecommunications Conference*, November 2004.

[17] K. Fall and K. Varadhan. ns notes and documentation. Technical report, UC Berkeley, LBL, USC/ISI, and Xerox PARC, November 1997.

[18] C. L. Fullmer and J. J. Garcia-Luna-Aceves. Floor acquisition multiple access (FAMA) for packet-radio networks. In *Proc. of ACM SIGCOMM*, pages 262–273, August 1995.

[19] C. L. Fullmer and J. J. Garcia-Luna-Aceves. Solutions to hidden terminal problems in wireless networks. In *Proc. of ACM SIGCOMM*, September 1997.

[20] A. E. Gamal, J. Mammen, B. Prabhakar, and D. Shah. Throughput-delay trade-off in wireless networks. In *Proc. of IEEE INFOCOM*, 2004.

[21] J. J. Garcia-Luna-Aceves and C. L. Fullmer. Floor acquisition multiple access (FAMA) in single-channel wireless networks. *Mobile Networks and Applications*, 4(3):157–174, 1999.

[22] M. Gastpar and M. Vetterli. On the capacity of wireless networks: The relay case. In *Proc. of IEEE INFOCOM*, 2002.

[23] M. Grossglauser and D. Tse. Mobility increases the capacity of ad-hoc wireless networks. In *Proc. of IEEE INFOCOM*, April 2001.

[24] P. Gupta and P. R. Kumar. The capacity of wireless networks. *IEEE Transactions on Information Theory*, 46(2):388–404, March 2000.

[25] Z. J. Haas and J. Deng. Dual busy tone multiple access (DBTMA): A multiple access control scheme for ad hoc networks. *IEEE Transactions on Communications*, 50(6):975–985, 2002.

[26] G. Holland, N. Vaidya, and P. Bahl. A rateadaptive MAC protocol for multihop wireless networks. In *ACM/IEEE International Conference on Mobile Computing and Networking*, July 2001.

[27] Eun-Sun Jung and N. H. Vaidya. A power control MAC protocol for ad hoc networks. In *ACM MOBICOM*, September 2002.

[28] R. Jurdak, C. V. Lopes, and P. Baldi. A survey, classification and comparative analysis of medium access control protocols for ad hoc networks. *IEEE Communications Surveys*, 6(1):2–16, First Quarter 2004.

[29] P. Karn. MACA: A new channel access protocol for packet radio. In *ARRL/CRRL Amateur Radio 9th Computer Networking Conference*, pages 134–140, 1990.

[30] L. Kleinrock and F. Tobagi. Random access techniques for data transmission over packet switched radio channels. In *Proc. of National Computer Conference*, pages 187–201, 1975.

[31] L. Kleinrock and F. A. Tobagi. Packet switching in radio channels: Part I–carrier sense multiple-access models and their throughput-delay characteristics. *IEEE Transactions on Communications*, 23(12):1400–1416, 1975.

[32] T. Kuang and C. Williamson. A bidirectional multi-channel MAC protocol for improving TCP performance on multihop wireless ad hoc networks. In *7th ACM International Symposium on Modeling, Analysis and Simulation of Wireless and Mobile Systems*, pages 301–310, 2004.

[33] J. Li, C. Blake, D. S. J. Couto, H. I. Lee, and R. Morris. Capacity of ad hoc wireless networks. In *Proc. of the Seventh Annual International Conference on Mobile Computing and Networking (MOBICOM)*, July 2001.

[34] K. Liu, T. Wong, J. Li, L. Bu, and J. Han. A reservation-based multiple access protocol with collision avoidance for wireless multihop ad hoc networks. In *Proc. of IEEE International Conference on Communications*, May 2003.

[35] J. Matousek and J. Nesetril. *Invitation to Discrete Mathematics*. Clarendon Press, Oxford, 1998.

[36] A. Muqattash and M. Krunz. CDMA-based MAC protocol for wireless ad hoc networks. In *4th ACM International Symposium on Mobile Ad Hoc Networking and Computing*, pages 153–164, 2003.

[37] R. Negi and A. Rajeswaran. Capacity of power constrained ad-hoc networks. In *Proc. of IEEE INFOCOM*, 2004.

[38] A. Okabe, B. Boots, and K. Sugihara. *Spatial Tessellations Concepts and Applications of Voronoi Diagrams.* Wiley, New York, 1992.

[39] R. Rao. Integration of on-demand service and route discovery in mobile ad hoc networks. Master's thesis, Department of Computer Science, North Carolina State University, 2004.

[40] V. Rodoplu and T. H. Meng. Bits-per-joule capacity of energy-limited wireless ad hoc networks. In *IEEE Global Telecommunications Conference*, volume 1, pages 16–20, November 2002.

[41] S. M. Ross. *Applied Probability Models with Optimization Application.* Holden-Day, San Francisco, 1970.

[42] E. M. Royer, P. M. Melliar-Smith, and L. E. Moser. An analysis of the optimum node density for ad hoc mobile networks. In *Proc. of IEEE International Conference on Communications*, June 2001.

[43] M. Sanchez, P. Manzoni, and Z. J. Haas. Determination of critical transmission range in ad hoc networks. In *Multiaccess Mobility and Teletraffic for Wireless Communications 1999 Workshop*, October 1999.

[44] S. Singh and C. Raghavendra. PAMAS: Power aware multi-access protocol with signalling for ad hoc networks. In *ACM SIGCOMM Computer Communication Review*, pages 5–26, 1998.

[45] N. Song, B. Kwak, J. Song, and L.E. Miller. Enhancement of IEEE 802.11 distributed coordination function with exponential increase exponential decrease backoff algorithm. In *Proc. of IEEE VTC*, April 2003.

[46] H. Takagi and L. Kleinrock. Optimal transmission ranges for randomly distributed packet radio terminals. *IEEE Transactions on Communications*, 32(3):246–257, March 1984.

[47] F. Talucci, M. Gerla, and L. Fratta. MACA-BI (MACA by invitation): A receiver-oriented access protocol for wireless multihop networks. In *Proc. of IEEE International Symposium on Personal, Indoor and Mobile Radio Communications Conference*, volume 2, pages 435–439, 1997.

[48] A. S. Tanenbaum. *Computer Networks*. Prentice Hall PTR, Upper Saddle River, NJ 07458, fourth edition, 2003.

[49] F. Tobagi and L. Kleinrock. Packet switching in radio channels: Part III–polling and (dynamic) split-channel reservation multiple access. *IEEE Transactions on Communications*, COM-24(8):832–844, August 1976.

[50] F. A. Tobagi and L. Kleinrock. Packet switching in radio channels: Part II–the hidden terminal problem in carrier sense multiple-access and the busy-tone solution. *IEEE Transactions on Communications*, 23(12):1417–1433, 1975.

[51] O. K. Tonguz and G. Ferrari. Is the number of neighbors in ad hoc wireless networks a good indicator of connectivity? In *Proc. of International Zurich Seminar on Communications*, pages 40–43, 2004.

[52] Yannis Viniotis. *Probability and Random Processes for Electrical Engineers*. McGraw-Hill Companies, Inc., 1998.

[53] Y. Wang and J. J. Garcia-Luna-Aceves. Collision avoidance in multi-hop ad hoc networks. In *Proc. of 10th IEEE International Symposium on Modeling, Analysis, and Simulation of Computer and Telecommunication Systems*, pages 145–154, October 2002.

[54] J. Weinmiller, M. Schlager, A. Festag, and A. Wolisz. Performance study of access

control in wireless LANs IEEE 802.11 DFWMAC and ETSI RES 10 HIPERLAN. *Mobile Networks and Applications*, 2:55–67, 1997.

[55] D. B. West. *Introduction to Graph Theory*. Prentice-Hall, Inc., second edition, 2001.

[56] IEEE 802.11 WG. Wireless lan medium access control (MAC) and physical-layer (PHY) specifications. 1999.

[57] C. Wu and V. Li. Receiver-initiated busy-tone multiple access in packet radio networks. In *Proc. of ACM SIGCOMM*, pages 336–342, 1988.

[58] H. Wu, S. Cheng, Y. Peng, K. Long, and J. Ma. IEEE 802.11 distributed coordination function (DCF): Analysis and enhancement. In *Proc. of IEEE International Conference on Communications*, April 2002.

[59] L. Wu and P. K. Varshney. Performance analysis of CSMA and BTMA protocols in multihop networks: (I)–single channel case. *Information Sciences*, 120(1-4):159–177, November 1999.

[60] S. L. Wu, C. Y. Lin, Y. C. Tseng, and J. P. Sheu. A new multi-channel MAC protocol with on-demand channel assignment for mobile ad hoc networks. In *International Symposium on Parallel Architectures, Algorithms and Networks (I-SPAN)*, pages 232–237, 2000.

[61] K. Xu, M. Gerla, and S. Bae. How effective is the IEEE 802.11 RTS/CTS handshake in ad hoc networks? In *IEEE Global Telecommunications Conference*, volume 1, pages 72–76, 2002.

[62] F. Xue and P. R. Kumar. The number of neighbors needed for connectivity of wireless networks. *Wireless Networks*, pages 169–181, April 2004.

[63] T. You, C. Yeh, and H. Hassanein. A new class of collision prevention MAC protocols for wireless ad hoc networks. In *Proc. of IEEE International Conference on Communications*, May 2003.

[64] H. Zhai and Y. Fang. Performance of wireless LANs based on IEEE 802.11 MAC protocols. In *Proc. of IEEE International Symposium on Personal, Indoor and Mobile Radio Communications Conference*, September 2003.

[65] H. Zhai, J. Wang, X. Chen, and Y. Fang. Medium access control in mobile ad hoc networks: Challenges and solutions. *Wireless Communications and Mobile Computing*, 2004.

[66] H. Zhai, J. Wang, Y. Fang, and D. Wu. A dual-channel MAC protocol for mobile ad hoc networks. In *IEEE Workshop on Wireless Ad Hoc and Sensor Networks, in conjuction with IEEE Globecom 2004*, November 2004.

[67] J. Zhang and W. K. G. Seah. Topology-based capacity analysis for ad hoc networks with end-to-end delay constraints. In *Proc. of the IEEE 6th Circuits and Systems Symposium on Emerging Technologies: Frontiers of Mobile and Wireless Communication*, volume 2, pages 541–544, May 2004.